

PAPER • OPEN ACCESS

Nanoparticles with cubic symmetry: classification of polyhedral shapes

To cite this article: Klaus E Hermann 2024 *J. Phys.: Condens. Matter* **36** 045303

View the [article online](#) for updates and enhancements.

You may also like

- [Right-angled polyhedra and hyperbolic 3-manifolds](#)
A. Yu. Vesnin
- [Algebraic methods for solution of polyhedra](#)
Idzhad Kh Sabitov
- [The atomic structure of ternary amorphous Ti_xSi_{1-x}O₂ hybrid oxides](#)
M Landmann, T Köhler, E Rauls et al.

Nanoparticles with cubic symmetry: classification of polyhedral shapes

Klaus E Hermann 

Theory Department, Fritz-Haber-Institut der Max-Planck-Gesellschaft, Faradayweg 4-6, 14195 Berlin, Germany

E-mail: hermann@fhi-berlin.mpg.de

Received 12 July 2023, revised 28 September 2023

Accepted for publication 9 October 2023

Published 30 October 2023



CrossMark

Abstract

Structural studies of polyhedral bodies can help to analyze geometric details of observed crystalline nanoparticles (NP) where we consider compact polyhedra of cubic point symmetry as simple models. Their surfaces are described by facets with normal vectors along selected Cartesian directions (a , b , c) together with their symmetry equivalents forming a direction family $\{abc\}$. Here we focus on polyhedra with facets of families $\{100\}$, $\{110\}$, and $\{111\}$, suggested for metal and oxide NPs with cubic lattices. Resulting generic polyhedra, cubic, rhombohedral, octahedral, and tetrahedral, have been observed as NP shapes by electron microscopy. They can serve for a complete description of non-generic polyhedra as intersections of corresponding generic species, not studied by experiment so far. Their structural properties are shown to be fully determined by only three parameters, facet distances R_{100} , R_{110} , and R_{111} of the three facet types. This provides a novel phase diagram to systematically classify all corresponding polyhedra. Their structural properties, such as shape, size, and facet geometry, are discussed in analytical and numerical detail with visualization of typical examples. The results may be used for respective NP simulations but also as a repository stimulating the structural interpretation of new NP shapes to be observed by experiment.

Supplementary material for this article is available [online](#)

Keywords: nanoparticles, cubic, symmetry, classification, polyhedral, shapes

1. Introduction

The detailed characterization of polyhedral bodies, while a subject of mathematical research since ancient times [1], has attracted new interest in connection with crystalline nanoparticles (NPs) [2–5]. These particles come in many sizes with disordered as well as polyhedral shapes. Their properties have been explored both experimentally and in theoretical studies due to their exciting physical and chemical behavior, which deviates often from that of corresponding bulk material [2–4].

Examples are applications in medicine [6–8], of magnetism [7–10], or in catalytic chemistry where metal and oxide NPs have become ubiquitous [11–18].

Many crystalline nano- and mesoscopic particles have been observed in experiments to exhibit polyhedral shape with flat local surface areas (facets) of high atom density, reminiscent of low Miller index planes of corresponding bulk crystal surfaces [10, 19, 20]. Their overall shape often reminds of compact sections confined by simple polyhedra where particles of material forming cubic bulk lattices [5, 19, 20] are found to exhibit, apart from hexagonal [21] and icosahedral geometry [22, 23], generic polyhedra of cubic symmetry, such as cubes and octahedra. Examples are NPs of metals, such as Au [24–26], Cu [26–28], Rh [17], Pd [14, 15, 17, 29], Pt [16, 17, 30], or of oxides and bromides, such as CeO₂ [31], Cu₂O [32], MgO [13], spinel Fe₃O₄ [7–9], CuBr [33], forming cubes



Original content from this work may be used under the terms of the [Creative Commons Attribution 4.0 licence](#). Any further distribution of this work must maintain attribution to the author(s) and the title of the work, journal citation and DOI.

and octahedra. Only selected other polyhedral shapes of cubic symmetry, like tetrahedral, have been observed for Pt NPs [10, 17, 18, 30, 34]. Here a systematic analysis of ideal polyhedra with cubic O_h symmetry as NP envelopes can be helpful to obtain further insight into possible NP shapes and their classification. Corresponding analytical results of the polyhedral structure allow estimates of NP sizes depending on the number of atoms included together with atom densities of the bulk material. They also give insight into the geometry of possible facets and their relative orientation at NP surfaces.

At an atomic scale, the facets of the NP surface join to form edges and corners whose detailed structure can, however, be rather complex. This is due to the discrete distribution of atom positions giving rise to corner capping with microfacets and edge flattening leading to microstrips as discussed earlier [5]. The perturbative effect is even enhanced by local relaxation at the particle surface and as a result of chemical surface reactions. However, for mesoscopic particles corner capping and edge flattening at an atomic scale is difficult to observe and is replaced by surface smoothing which extends over many atom layers.

In the present work, extending previous theoretical analyses [5, 35], we focus on geometrical details of polyhedra of cubic O_h symmetry with their symmetry center at the origin of a Cartesian coordinate system. The polyhedral surfaces can be described by facets representing planar sections with normal vectors along selected Cartesian directions (a, b, c) together with their O_h symmetry equivalents. For NPs of metals, oxides and other material with cubic lattice geometry, possible facets are observed to represent sections of high-density monolayers of the cubic bulk, characterized by Miller index families $\{hkl\} = \{100\}, \{110\},$ and $\{111\}$ [20], which seem to be energetically preferred. This suggests polyhedra with facet normal vectors $(a, b, c) = (1, 0, 0), (1, 1, 0),$ and $(1, 1, 1)$ together with their O_h symmetry equivalents. The analysis reveals different types of generic polyhedra which can serve for the definition of general polyhedra described as intersections of corresponding generic species. Their structural properties, such as shape, size, and surface facets, are shown to be fully determined by only three structure parameters, the facet distances $R_{100}, R_{110}, R_{111}$. In fact, all polyhedral shapes, independent of size, can already be characterized by only two relative facet distances, such as $x_{110} = \sqrt{2} R_{110}/R_{100}$ and $x_{111} = \sqrt{3} R_{111}/R_{100}$, which provides a novel phase diagram of all polyhedral shapes, allowing a systematic classification of all compact polyhedra of cubic symmetry exhibiting facets of direction families $\{100\}, \{110\},$ and $\{111\}$. The continuous variation of the three structure parameters leads to a simplified mathematical description of possible shapes of cubic nano- and meso-size particles as compared to a more complex discrete structural description published earlier [5].

We also consider generic polyhedra of O_h symmetry which are confined by facets of one general direction family $\{abc\}$, yielding up to 48 different facet directions. These hexoctahedral polyhedra can be used to model cubic NPs with higher Miller index facets reflecting sections of stepped and kinked facet surfaces [20], also observed in some cases by electron microscopy [18, 34]. Clearly, their structural properties are

fully described by a facet distance R_{abc} and all facet indices, a, b, c , determining the corresponding facet normal vector family.

All structural results of the present polyhedra are discussed in analytical and numerical detail with visualization [36] of characteristic examples. The different sections are structured identically and presented in parts with very similar phrasing to enable easy comparison. Section 2 introduces notations and definitions used to characterize polyhedral shape while section 3 discusses results for generic and non-generic polyhedra in detail. Finally, section 4 summarizes conclusions from the present work. The supplement provides further details to complement results discussed in section 3.

Altogether, the present analysis offers a sound basis to describe compact polyhedra of cubic symmetry which may be used as a repository available for NP simulations. It can help the interpretation of structures of real compact NPs observed by experiment and can also stimulate further experimental research on nano- and meso-size particle structures not identified so far.

2. Notation and formal definitions

We consider compact polyhedra of central O_h symmetry confined by finite sections of planes (facets) which can be described by facet normal vectors \underline{e}_{abc} and facet distances R_{abc} from the polyhedral center, resulting in facet vectors

$$\underline{R}_{abc} = R_{abc}\underline{e}_{abc}, \quad \underline{e}_{abc} = 1/w(a,b,c), \quad w = \sqrt{a^2 + b^2 + c^2}, \quad (1)$$

with \underline{e}_{abc} described by facet indices a, b, c in Cartesian coordinates relative to the polyhedral center. Due to the polyhedral O_h symmetry, each facet normal vector \underline{e}_{abc} implies a number of symmetry equivalents $\underline{e}_{a'b'c'}$ originating from all O_h symmetry operations applied to \underline{e}_{abc} . Together with \underline{e}_{abc} , this forms a family of symmetry equivalent facet normal vectors, denoted $\underline{e}_{\{abc\}}$ in the following and corresponding to a direction family defined as $\{abc\}$. (Note that in the following we use a short hand notation taken from crystallography [20]: curly brackets $\{\dots\}$ to indicate facet normal direction families with all members and normal brackets (\dots) referring to specific directions.)

In the most general case, applying all 48 O_h symmetry operations to a vector \underline{e}_{abc} , where $a, b,$ and c are all finite and different from each other yields a direction family $\{abc\}$ of 48 members described by

$$\begin{aligned} \underline{e}_{\{abc\}} = & 1/w(\pm a, \pm b, \pm c), 1/w(\pm a, \pm c, \pm b), \\ & 1/w(\pm b, \pm a, \pm c), 1/w(\pm b, \pm c, \pm a) \\ & 1/w(\pm c, \pm a, \pm b), 1/w(\pm c, \pm b, \pm a). \end{aligned} \quad (2a)$$

Special cases resulting in direction families $\{100\}, \{110\}, \{111\}$ are

$$\underline{e}_{\{100\}} = (\pm 1, 0, 0), (0, \pm 1, 0), (0, 0, \pm 1), \quad (2b)$$

$$\underline{e}_{\{110\}} = 1/\sqrt{2} (\pm 1, \pm 1, 0), 1/\sqrt{2} (\pm 1, 0, \pm 1),$$

$$1/\sqrt{2} (0, \pm 1, \pm 1) \quad (2c)$$

$$\underline{e}_{\{111\}} = 1/\sqrt{3} (\pm 1, \pm 1, \pm 1) \quad (2d)$$

which yield smaller families of 6, 12, and 8 members, respectively.

As a result of the O_h symmetry, polyhedral facets appear always as parallel pairs with facet vectors $\pm \underline{R}_{abc}$ on opposite sides of the polyhedron. This leads to polyhedral diameters $D_{abc} = 2R_{abc}$ characterizing the size of the polyhedron. Altogether, the most general polyhedra of O_h symmetry can be denoted by

$$P(\underline{R}_{\{abc\}}; \underline{R}_{\{a'b'c'\}}; \underline{R}_{\{a''b''c''\}}; \dots)$$

$$= P(R_{abc}, \{abc\}; R_{a'b'c'}, \{a'b'c'\}; R_{a''b''c''}, \{a''b''c''\}; \dots) \quad (3)$$

depending on the number of different facet types. Here we distinguish between *generic* and *non-generic* species where generic polyhedra are defined by facets of only one direction family $\{abc\}$ whereas non-generic polyhedra include several different direction families as noted in definition (3).

The above notations and definitions will be used in the following discussion. Note that some of the expressions of corner coordinates in section 3.2 use auxiliary parameters g, h which are defined separately for each section.

3. Discussion

3.1. Generic polyhedra

Generic polyhedra are confined by facets of only one direction family $\{abc\}$ and are denoted $P(\underline{R}_{\{abc\}})$. Here the simplest examples are those for $\{abc\} = \{100\}, \{110\},$ and $\{111\}$ which will be discussed before the general case $\{abc\}$, which includes also the simple examples, is treated in detail.

3.1.1. Cubic polyhedra $P(\underline{R}_{\{100\}})$. Cubic polyhedra have been observed in experiments on numerous nano- and mesoscopic particles, including metallic (e.g. Cu [26–28], Au [25], Pt [16]) and oxidic (e.g. Cu_2O [32], Fe_3O_4 [7–10], MgO [13]). According to (2b) and (3), these polyhedra are confined by all 6 $\{100\}$ facets with facet distances R_{100} defining, as expected, the cubic polyhedron, see figure 1(a).

The 8 polyhedral corners are described by vectors $\underline{C}_{\{111\}}$ relative to the center where in Cartesian coordinates

$$\underline{C}_{\{111\}} = R_{100} (\pm 1, \pm 1, \pm 1). \quad (4)$$

Euler's polyhedron rule [1] states that the numbers of corners N_c , facets N_f , and edges N_e of a convex polyhedron are related by

$$N_c + N_f - N_e = 2. \quad (5)$$

This yields $P(\underline{R}_{\{100\}})$ with corners connected by 12 (8 + 6-2) edges, see figure 1(a).

An analysis shows that all 6 facets are of the same square shape where each $\{100\}$ facet extends between four adjacent corners $\underline{C}_{\{111\}}$, such as $\underline{C}_{(111)}, \underline{C}_{(-111)}, \underline{C}_{(1-11)}, \underline{C}_{(-1-11)}$. The resulting four edges connect corners, such as $\underline{C}_{(111)}$ with $\underline{C}_{(-111)}$, at distances d_{a1} given by

$$d_{a1} = 2R_{100}. \quad (6)$$

The largest distance from the polyhedral center to its surface along (a, b, c) directions, $s_{abc}(R_{100})$, is given by

$$s_{100}(R_{100}) = R_{100} \quad (7a)$$

$$s_{110}(R_{100}) = \sqrt{2}R_{100} \quad (7b)$$

$$s_{111}(R_{100}) = \sqrt{3}R_{100}. \quad (7c)$$

Further, the area of each facet is given by F_0 with

$$F_0 = \left| \left(\underline{C}_{(-111)} - \underline{C}_{(111)} \right) \times \left(\underline{C}_{(1-11)} - \underline{C}_{(111)} \right) \right| = 4R_{100}^2. \quad (8)$$

Thus, the total facet surface, F_{surf} (sum over all facet areas) and the volume V_{tot} of the polyhedron are given by

$$F_{\text{surf}} = 6F_0 = 24R_{100}^2 \quad (9)$$

$$V_{\text{tot}} = F_{\text{surf}}R_{100}/3 = 8R_{100}^3. \quad (10)$$

Figure 1(b) shows a NP of atom balls representing a simple cubic (sc) crystal section where a polyhedron $P(\underline{R}_{\{100\}})$ serves as envelope with its corners $\underline{C}_{\{111\}}$ coinciding with atom sites.

3.1.2. Rhombohedral polyhedra $P(\underline{R}_{\{110\}})$. Rhombohedral polyhedra have been mentioned in the experimental literature [18, 34] but clear particle images do not seem to exist so far. According to (2c) and (3), these polyhedra are confined by all 12 $\{110\}$ facets with facet distances R_{110} defining the rhombohedral polyhedron, see figure 2(a).

The 14 polyhedral corners fall in two groups of 6 and 8 each, described by vectors $\underline{C}_{\{100\}}$ and $\underline{C}_{\{111\}}$ relative to the center, where in Cartesian coordinates

$$\underline{C}_{\{100\}} = \sqrt{2}R_{110} (\pm 1, 0, 0), = \sqrt{2}R_{110} (0, \pm 1, 0),$$

$$= \sqrt{2}R_{110} (0, 0, \pm 1) \quad (11a)$$

$$\underline{C}_{\{111\}} = 1/\sqrt{2}R_{110} (\pm 1, \pm 1, \pm 1). \quad (11b)$$

With $P(\underline{R}_{\{110\}})$ yielding 12 facets and 14 corners the number of its polyhedral edges amounts to 24 according to (5), see figure 2(a).

An analysis shows that all 12 facets are of the same rhombic shape where each $\{110\}$ facet extends between adjacent corners $\underline{C}_{\{100\}}$ and $\underline{C}_{\{111\}}$, such as $\underline{C}_{(100)}, \underline{C}_{(111)}, \underline{C}_{(001)}$,

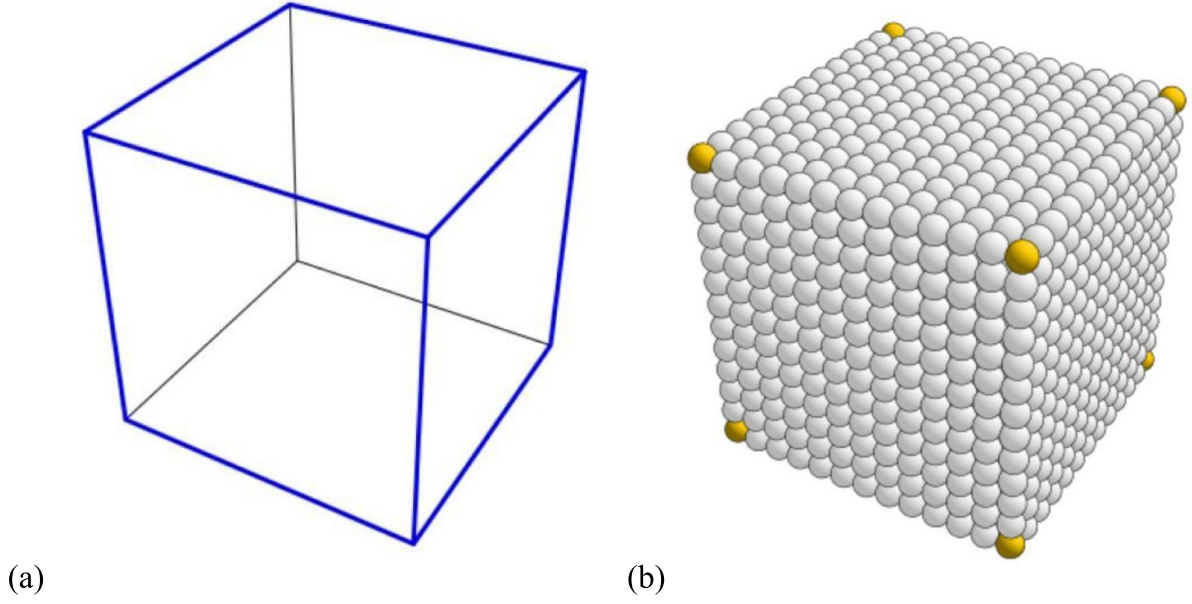


Figure 1. (a) Sketch of generic cubic polyhedron $P(R_{\{100\}})$ with front facets in blue and back facets in black. (b) Nanoparticle of gray atom balls of a sc crystal section filling the polyhedron, see text. Yellow balls correspond to corners $\underline{C}_{\{111\}}$ which coincide with atom sites.

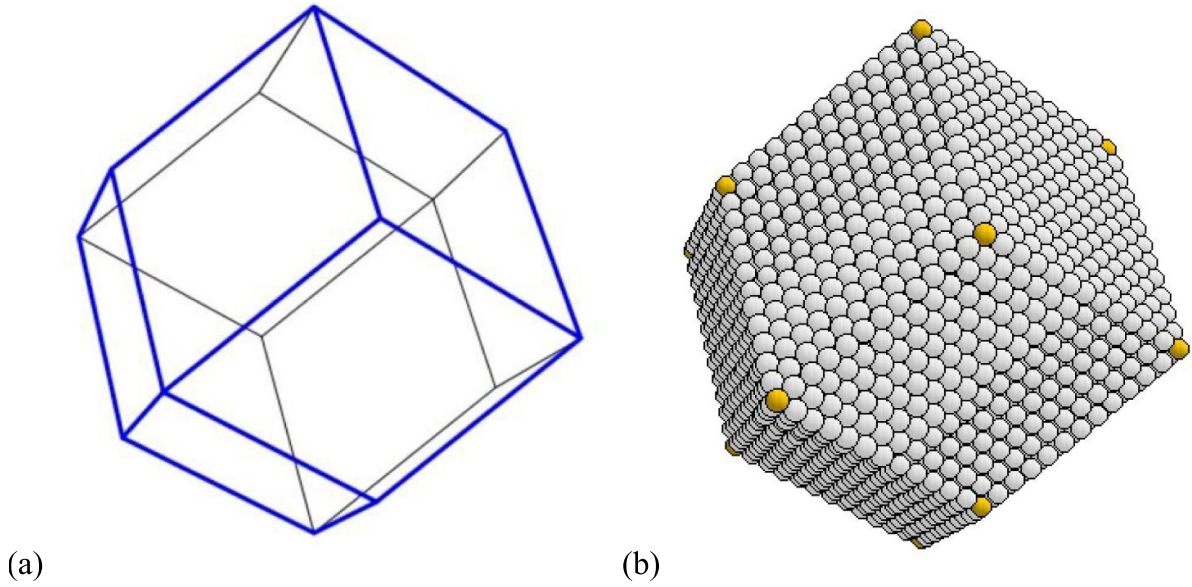


Figure 2. (a) Sketch of generic rhombohedral polyhedron $P(R_{\{110\}})$ with front facets in blue and back facets in black. (b) Nanoparticle of gray atom balls of a bcc lattice section filling the polyhedron. Yellow balls correspond to corners $\underline{C}_{\{100\}}$ and $\underline{C}_{\{111\}}$ which coincide with atom sites.

$\underline{C}_{(1-11)}$. The resulting four edges connect corners, such as $\underline{C}_{(100)}$ with $\underline{C}_{(111)}$, at distances d_{b1} given by

$$d_{b1} = \sqrt{(3/2)} R_{110}. \quad (12)$$

Thus, the polyhedron can be described as a rhombic dodecahedron reminding of the shape of Wigner–Seitz cells of the face-centered cubic (fcc) crystal lattice [37].

The largest distance from the polyhedral center to its surface along (a, b, c) directions, $s_{abc}(R_{110})$, is given by

$$s_{100}(R_{110}) = \sqrt{2} R_{110} \quad (13a)$$

$$s_{110}(R_{110}) = R_{110} \quad (13b)$$

$$s_{111}(R_{110}) = \sqrt{(3/2)} R_{110}. \quad (13c)$$

Further, the area of each facet is given by F_0 with

$$F_0 = \left| \left(\underline{C}_{(001)} - \underline{C}_{(111)} \right) \times \left(\underline{C}_{(100)} - \underline{C}_{(111)} \right) \right| = \sqrt{2} R_{110}^2. \quad (14)$$

Thus, the total facet surface, F_{surf} (sum over all facet areas) and the volume V_{tot} of the polyhedron are given by

$$F_{\text{surf}} = 12F_0 = 12\sqrt{2}R_{110}^2 \quad (15)$$

$$V_{\text{tot}} = F_{\text{surf}}R_{110}/3 = 4\sqrt{2}R_{110}^3. \quad (16)$$

Figure 2(b) shows a NP of atom balls representing a body-centered cubic (bcc) crystal section where a polyhedron $P(\underline{R}_{\{110\}})$ serves as envelope with its corners $\underline{C}_{\{100\}}$ and $\underline{C}_{\{111\}}$ coinciding with atom sites.

3.1.3. Octahedral polyhedra $P(\underline{R}_{\{111\}})$. Octahedral polyhedra have been observed in experiments on numerous nano- and mesoscopic particles, including metallic (e.g. Cu [28], Pd [14, 15, 29], Au [24, 25], Pt [16]) and oxidic (e.g. Cu₂O [28, 32], CeO₂ [31], MgO [13]). According to (2d) and (3), these polyhedra are confined by all 8 $\{111\}$ facets with facet distances R_{111} defining the octahedral polyhedron, see figure 3(a).

The 6 polyhedral corners are described by vectors $\underline{C}_{\{100\}}$ relative to the center where in Cartesian coordinates

$$\begin{aligned} \underline{C}_{\{100\}} &= \sqrt{3}R_{111}(\pm 1, 0, 0), \quad = \sqrt{3}R_{111}(0, \pm 1, 0), \\ &= \sqrt{3}R_{111}(0, 0, \pm 1). \end{aligned} \quad (17)$$

With $P(\underline{R}_{\{111\}})$ yielding 8 facets and 6 corners the number of its polyhedral edges amounts to 12 according to (5), see figure 3(a).

An analysis shows that all 8 facets are of the same equilateral triangular shape where each $\{111\}$ facet extends between adjacent corners $\underline{C}_{\{100\}}$, such as $\underline{C}_{(100)}$, $\underline{C}_{(010)}$, $\underline{C}_{(001)}$. The resulting three edges connect corners, such as $\underline{C}_{(010)}$ with $\underline{C}_{(100)}$, at distances d_{c1} given by

$$d_{c1} = \sqrt{6}R_{111}. \quad (18)$$

The largest distance from the polyhedral center to its surface along (a, b, c) directions, $s_{abc}(R_{111})$, is given by

$$s_{100}(R_{111}) = \sqrt{3}R_{111} \quad (19a)$$

$$s_{110}(R_{111}) = \sqrt{(3/2)}R_{111} \quad (19b)$$

$$s_{111}(R_{111}) = R_{111}. \quad (19c)$$

Further, the area of each facet is given by F_0 with

$$\begin{aligned} F_0 &= 1/2 \left| \left(\underline{C}_{(100)} - \underline{C}_{(001)} \right) \times \left(\underline{C}_{(010)} - \underline{C}_{(001)} \right) \right| \\ &= (3/2)\sqrt{3}R_{111}^2. \end{aligned} \quad (20)$$

Thus, the total facet surface, F_{surf} (sum over all facet areas) and the volume V_{tot} of the polyhedron are given by

$$F_{\text{surf}} = 8F_0 = 12\sqrt{3}R_{111}^2 \quad (21)$$

$$V_{\text{tot}} = F_{\text{surf}}R_{111}/3 = 4\sqrt{3}R_{111}^3. \quad (22)$$

Figure 3(b) shows a NP of atom balls representing a fcc crystal section where a polyhedron $P(\underline{R}_{\{111\}})$ serves as envelope with its corners $\underline{C}_{\{100\}}$ coinciding with atom sites.

3.1.4. Hexoctahedral polyhedra $P(\underline{R}_{\{abc\}})$. Hexoctahedral polyhedra (including trisoctahedral, trapezohedral, and tetrahexahedral) have been discussed in the literature but only in a few cases (Pd [18], Pt [18, 30, 34]) been observed. A systematic classification, discussed in section S.1 of the supplement, seems to be missing. According to (2a) and (3), these polyhedra are confined by up to 48 elementary $\{abc\}$ facets with facet distances R_{abc} . If values of a, b, c coincide or equal zero, different elementary facets can join to yield larger faces and the number of facet normal vectors decreases to 24, 12, 8, or 6 facets as discussed in section S.1 of the supplement. Here we focus on the general case of $a > b > c > 0$ which results in 48 different $\{abc\}$ facets, see figure 4(a).

As a result of the overall O_h symmetry of the $P(\underline{R}_{\{abc\}})$ polyhedron, its corners can appear only along selected directions from the center given by vectors $\underline{e}_{\{100\}}$, $\underline{e}_{\{110\}}$, $\underline{e}_{\{111\}}$ according to (2b)–(2d). This yields possible corner vectors

$$\underline{C}_{\{hkl\}} = p_{hkl}\underline{e}_{\{hkl\}}, \quad \{hkl\} = \{100\}, \{110\}, \{111\} \quad (23)$$

where $\underline{C}_{\{hkl\}}$ must point to several joining $\{abc\}$ facets. This requires that

$$\begin{aligned} \underline{C}_{\{hkl\}}\underline{e}_{\{abc\}} &= p_{hkl} \left(\underline{e}_{\{hkl\}}\underline{e}_{\{abc\}} \right) = R_{abc}, \\ p_{hkl} &= R_{abc} / \left(\underline{e}_{\{hkl\}}\underline{e}_{\{abc\}} \right). \end{aligned} \quad (24)$$

Together with (2a)–(2d) we obtain

$$\underline{e}_{\{100\}}\underline{e}_{\{abc\}} = a/w, \quad \underline{C}_{\{100\}} = R_{abc}w/a\underline{e}_{\{100\}} \quad (25a)$$

$$\underline{e}_{\{110\}}\underline{e}_{\{abc\}} = (a+b)/(\sqrt{2}w), \quad \underline{C}_{\{110\}} = R_{abc}w\sqrt{2}/(a+b)\underline{e}_{\{110\}} \quad (25b)$$

$$\begin{aligned} \underline{e}_{\{111\}}\underline{e}_{\{abc\}} &= (a+b+c)/(\sqrt{3}w), \\ \underline{C}_{\{111\}} &= R_{abc}w\sqrt{3}/(a+b+c)\underline{e}_{\{111\}} \end{aligned} \quad (25c)$$

describing, altogether, 26 different corners. With $P(\underline{R}_{\{abc\}})$ yielding 48 facets and 26 corners the number of its polyhedral edges amounts to 72 according to (5), see figure 4(a).

An analysis shows that all 48 $\{abc\}$ facets are of triangular shape. There are two sets of 24 identical facets each where the facets of the second set are obtained as mirror images of those of the first. Each facet triangle extends between adjacent corners $\underline{C}_{\{100\}}$, $\underline{C}_{\{110\}}$, and $\underline{C}_{\{111\}}$, such as $\underline{C}_{(100)}$, $\underline{C}_{(110)}$, $\underline{C}_{(111)}$. The resulting three edges connect corners $\underline{C}_{\{100\}}$ with $\underline{C}_{\{110\}}$, $\underline{C}_{\{100\}}$ with $\underline{C}_{\{111\}}$, and $\underline{C}_{\{110\}}$ with $\underline{C}_{\{111\}}$, at different distances d_{d1} , d_{d2} , and d_{d3} given by

$$d_{d1} = R_{abc}w\sqrt{(a^2 + b^2)} / [a(a+b)] \quad (26a)$$

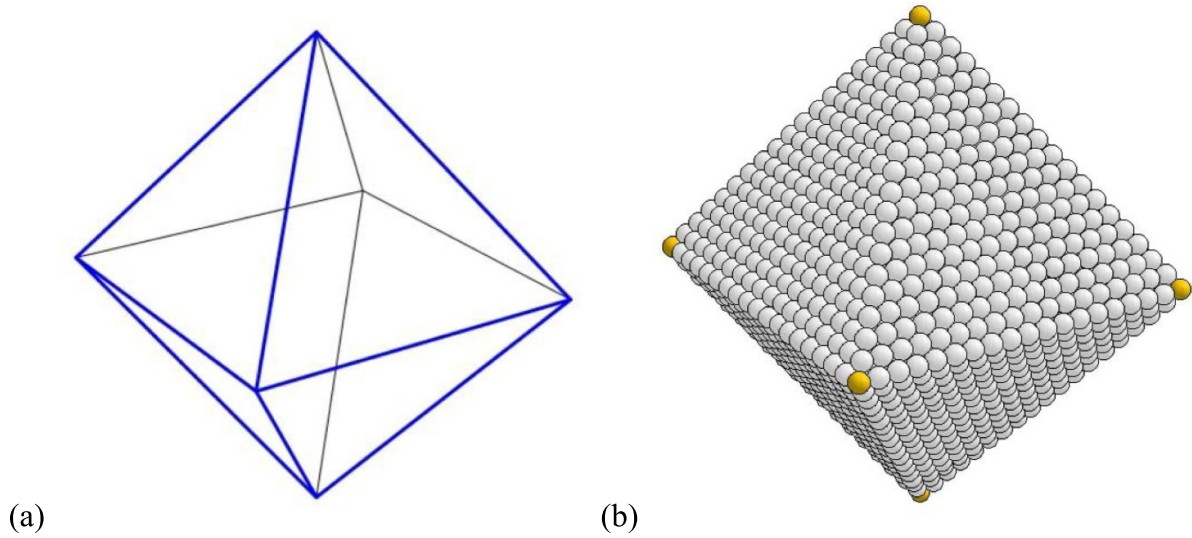


Figure 3. (a) Sketch of generic octahedral polyhedron $P(\underline{R}_{\{111\}})$ with front facets in blue and back facets in black. (b) Nanoparticle of gray atom balls of an fcc lattice section filling the polyhedron. Yellow balls correspond to corners $\underline{C}_{\{100\}}$ which coincide with atom sites.

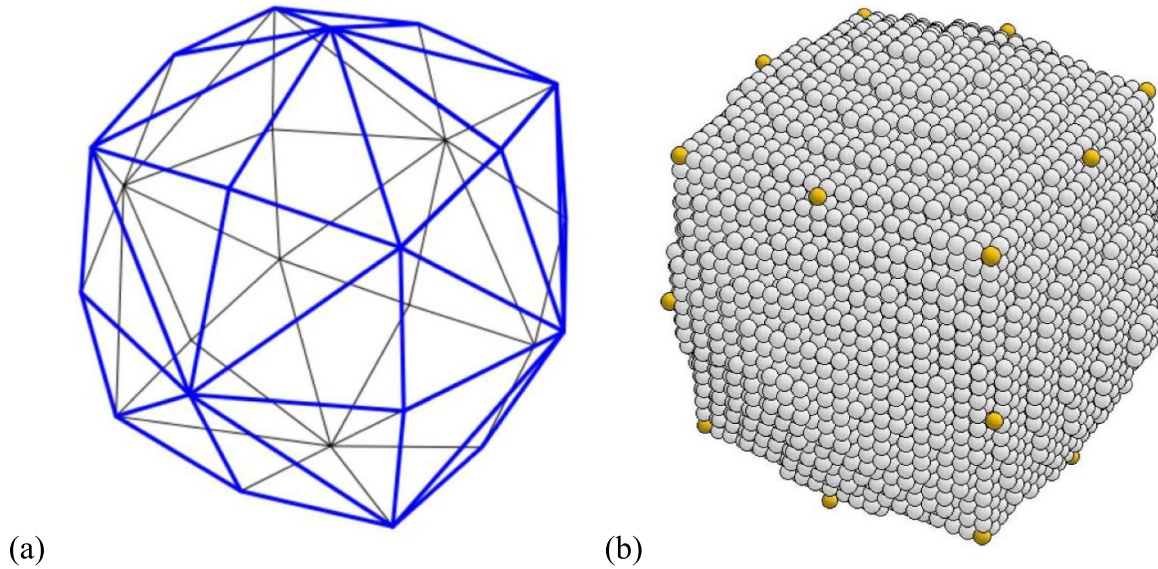


Figure 4. (a) Sketch of polyhedron $P(\underline{R}_{\{abc\}})$ for $a = 7, b = 3, c = 1$ with front facets in blue and back facets in black. (b) Nanoparticle of gray atom balls of a sc lattice section filling the polyhedron. Yellow balls correspond to corners $\underline{C}_{\{110\}}$ and $\underline{C}_{\{111\}}$ which coincide with atom sites.

$$d_{d2} = R_{abc}w\sqrt{[2a^2 + (b+c)^2]} / [a(a+b+c)] \quad (26b)$$

$$d_{d3} = R_{abc}w\sqrt{[(a+b)^2 + 2c^2]} / [(a+b)(a+b+c)]. \quad (26c)$$

Further, the area of each facet is given by F_0 with

$$F_0 = 1/2 | (C_{\{110\}} - C_{\{100\}}) \times (C_{\{111\}} - C_{\{100\}}) | \\ = 1/2 (R_{abc}w)^2 w / [a(a+b)(a+b+c)]. \quad (27)$$

Thus, the total facet surface, F_{surf} (sum over all facet areas) and the volume V_{tot} of the polyhedron are given by

$$F_{\text{surf}} = 48 F_0 = 24 (R_{abc}w)^2 w / [a(a+b)(a+b+c)] \quad (28)$$

$$V_{\text{tot}} = F_{\text{surf}}R_{abc}/3 = 8 (R_{abc}w)^3 / [a(a+b)(a+b+c)]. \quad (29)$$

Figure 4(b) shows a NP of atom balls representing a sc crystal section where a polyhedron $P(\underline{R}_{\{abc\}})$ serves as envelope with its corners $\underline{C}_{\{110\}}$ and $\underline{C}_{\{111\}}$ coinciding with atom sites. Note that polyhedral corners $\underline{C}_{\{100\}}$ do not appear due to the discrete distribution of the atom sites. The figure also illustrates the stepped/kinked structure of the different facet areas.

Other polyhedra $P(\underline{R}_{\{a'b'c'\}})$ of O_h symmetry, where components $a', b',$ and c' are not subject to constraints $a' > b' > c' > 0$ imposed in this section, can be treated completely analogous to the present discussion. First, we note that if a', b', c' are permutations of facet indices a, b, c the polyhedra $P(\underline{R}_{\{a'b'c'\}})$ and $P(\underline{R}_{\{abc\}})$ are identical in shape. Second,

mirror symmetry requires that if any of the components a' , b' , c' is negative it can be replaced by the corresponding positive value without affecting the polyhedron shape. Thus, a' , b' , c' can always be regrouped and its component values inverted to yield a , b , c with $a \geq b \geq c \geq 0$ while conserving the polyhedron shape. So far, we focused on polyhedra $P(\underline{R}_{\{abc\}})$ where equality and zero values of the facet indices a , b , c are ignored. However, all other cases, including $P(\underline{R}_{\{100\}})$, $P(\underline{R}_{\{110\}})$, and $P(\underline{R}_{\{111\}})$ of sections 3.1.1–3, are discussed in section S.1 of the supplement.

3.2. Non-generic polyhedra

Non-generic polyhedra of O_h symmetry $P(\underline{R}_{\{abc\}}; \underline{R}_{\{a'b'c'\}}; \dots)$ show facets with orientations of more than one family of facet vectors $\underline{R}_{\{abc\}}$. This can be considered as combining confinements of corresponding different generic polyhedra $P(\underline{R}_{\{abc\}})$, discussed in section 3.1, which share their symmetry center. Thus, non-generic polyhedra represent mutual intersections of more than one generic polyhedron, where one cuts corners and edges of the other(s) to form additional facets.

In this section we restrict ourselves to non-generic polyhedra with up to three selected generic polyhedra, cubic $P(\underline{R}_{\{100\}})$, rhombohedral $P(\underline{R}_{\{110\}})$, and octahedral $P(\underline{R}_{\{111\}})$, which offer $\{100\}$, $\{110\}$, as well as $\{111\}$ facets with facet distances R_{100} , R_{110} , and R_{111} . This choice is motivated by the structure of ideal cubic NPs whose bulk atoms form sections of cubic crystals (simple, face-, or body-centered) and where corresponding facets of $\{100\}$, $\{110\}$, and $\{111\}$ families reflect crystal monolayers of highest atom density [20].

The corresponding facet distances R_{100} , R_{110} , and R_{111} can be considered as structure parameters, defining the present non-generic polyhedra, and their relations with each other determine the polyhedral shape. In the following, we discuss the three types of polyhedra, which combine two generic polyhedra each, i.e. $P(\underline{R}_{\{100\}}; \underline{R}_{\{110\}})$, $P(\underline{R}_{\{100\}}; \underline{R}_{\{111\}})$, and $P(\underline{R}_{\{110\}}; \underline{R}_{\{111\}})$ in sections 3.2.1–3, before we consider the most general case of polyhedra as intersections of three generic polyhedra, $P(\underline{R}_{\{100\}}; \underline{R}_{\{110\}}; \underline{R}_{\{111\}})$, in section 3.2.4.

3.2.1. Cubo-rhombic polyhedra $P(\underline{R}_{\{100\}}; \underline{R}_{\{110\}})$. Non-generic polyhedra $P(\underline{R}_{\{100\}}; \underline{R}_{\{110\}})$, denoted *cubo-rhombic*, represent intersections of two generic polyhedra, cubic $P(\underline{R}_{\{100\}})$ and rhombohedral $P(\underline{R}_{\{110\}})$, see figure 5. If the edges of the cubic polyhedron $P(\underline{R}_{\{100\}})$ lie inside the rhombohedral polyhedron $P(\underline{R}_{\{110\}})$, the resulting combination $P(\underline{R}_{\{100\}}; \underline{R}_{\{110\}})$ will be generic cubic. This requires

$$s_{110}(R_{100}) \leq s_{110}(R_{110}). \quad (30)$$

and according to (7b) and (13b)

$$R_{110} \geq \sqrt{2}R_{100}. \quad (31)$$

On the other hand, if the corners of the rhombohedral polyhedron $P(\underline{R}_{\{110\}})$ lie inside the cubic polyhedron $P(\underline{R}_{\{100\}})$, the

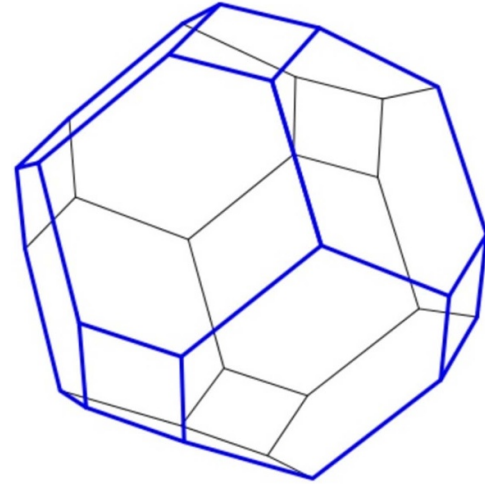


Figure 5. Sketch of cubo-rhombic polyhedron $P(\underline{R}_{\{100\}}; \underline{R}_{\{110\}})$, $R_{110}/R_{100} = 0.864$, with front facets in blue and back facets in black.

resulting combination $P(\underline{R}_{\{100\}}; \underline{R}_{\{110\}})$ will be generic rhombohedral. This requires

$$s_{100}(R_{110}) \leq s_{100}(R_{100}) \quad (32)$$

and according to (7a) and (13a)

$$R_{110} \leq 1/\sqrt{2}R_{100}. \quad (33)$$

Thus, the two generic polyhedra intersect and yield a true non-generic polyhedron $P(\underline{R}_{\{100\}}; \underline{R}_{\{110\}})$ with both $\{100\}$ and $\{110\}$ facets only for facet distances R_{100} , R_{110} with

$$1/\sqrt{2}R_{100} < R_{110} < \sqrt{2}R_{100} \quad (34)$$

while $P(\underline{R}_{\{100\}}; \underline{R}_{\{110\}})$ is generic cubic for $R_{110} \geq \sqrt{2}R_{100}$ and generic rhombohedral for $R_{110} \leq 1/\sqrt{2}R_{100}$. As a consequence, generic polyhedra $P(\underline{R}_{\{100\}})$ and $P(\underline{R}_{\{110\}})$ can be described alternatively by non-generic $P(\underline{R}_{\{100\}}; \underline{R}_{\{110\}})$ where

$$P(\underline{R}_{\{100\}}) = P(\underline{R}_{\{100\}}; \underline{R}_{\{110\}}) \text{ with } R_{110} \geq \sqrt{2}R_{100} \text{ (cubic)} \quad (35a)$$

$$P(\underline{R}_{\{110\}}) = P(\underline{R}_{\{100\}}; \underline{R}_{\{110\}}) \text{ with } R_{100} \geq \sqrt{2}R_{110} \text{ (rhombohedral)} \quad (35b)$$

The surfaces of general cubo-rhombic polyhedra $P(\underline{R}_{\{100\}}; \underline{R}_{\{110\}})$ exhibit 6 $\{100\}$ facets and 12 $\{110\}$ facets as shown in figure 5.

There are 32 polyhedral corners which can be evaluated by methods described in section S.3 of the supplement. They fall into two groups of 24 and 8 corners each, described by vectors $\underline{C}_{\{1hh\}}$ and $\underline{C}_{\{111\}}$ relative to the center, where in Cartesian coordinates

$$\begin{aligned} \underline{C}_{\{1hh\}} &= R_{100} (\pm 1, \pm h, \pm h), = R_{100} (\pm h, \pm 1, \pm h), \\ &= R_{100} (\pm h, \pm h, \pm 1) \\ \underline{C}_{\{111\}} &= 1/\sqrt{2} R_{110} (\pm 1, \pm 1, \pm 1), \quad h = \sqrt{2} R_{110}/R_{100} - 1, \\ &0 \leq h \leq 1. \end{aligned} \quad (36)$$

The 6 {100} facets are of the same square shape where each facet extends between four adjacent corners $\underline{C}_{\{1hh\}}$, such as $\underline{C}_{(1hh)}$, $\underline{C}_{(1-hh)}$, $\underline{C}_{(1-h-h)}$, $\underline{C}_{(1h-h)}$. The resulting four edges connect corners, such as $\underline{C}_{(1hh)}$ with $\underline{C}_{(1-hh)}$, at distances d_{e1} given by

$$d_{e1} = 2 \left(\sqrt{2} R_{110} - R_{100} \right). \quad (37)$$

The 12 {110} facets are of the same hexagonal shape where each facet extends between six adjacent corners $\underline{C}_{\{1hh\}}$ and $\underline{C}_{\{111\}}$, such as $\underline{C}_{(1hh)}$, $\underline{C}_{(1-hh)}$, $\underline{C}_{(1-11)}$, $\underline{C}_{(h-h1)}$, $\underline{C}_{(hh1)}$, $\underline{C}_{(111)}$. Of the resulting six edges two connect corners, such as $\underline{C}_{(1hh)}$ with $\underline{C}_{(1-hh)}$, at distances d_{e1} according to (37) while four connect corners, such as $\underline{C}_{(1hh)}$ with $\underline{C}_{(111)}$, at distances d_{e2} given by

$$d_{e2} = \sqrt{3/2} \left(\sqrt{2} R_{100} - R_{110} \right). \quad (38)$$

The largest distance from the polyhedral center to its surface along (a, b, c) directions, $s_{abc}(R_{100}, R_{110})$, is given by

$$s_{100}(R_{100}, R_{110}) = R_{100} \quad (39a)$$

$$s_{110}(R_{100}, R_{110}) = R_{110} \quad (39b)$$

$$s_{111}(R_{100}, R_{110}) = \sqrt{3/2} R_{110}. \quad (39c)$$

Further, the area of each square {100} facet is given by F_0 where with (37)

$$F_0 = 4 \left(\sqrt{2} R_{110} - R_{100} \right)^2 \quad (40)$$

and of each hexagonal {110} facet by F_1 where with (14)

$$F_1 = \sqrt{2} \left(\sqrt{2} R_{100} - R_{110} \right) \left(3R_{110} - \sqrt{2} R_{100} \right). \quad (41)$$

This yields the total facet surface, F_{surf} (sum over all facet areas) and the volume V_{tot} of the polyhedron according to

$$F_{\text{surf}} = 6F_0 + 12F_1 \quad (42)$$

$$V_{\text{tot}} = (6F_0 R_{100} + 12F_1 R_{110})/3. \quad (43)$$

3.2.2. Cubo-octahedral polyhedra $P(\underline{R}_{\{100\}}; \underline{R}_{\{111\}})$. Non-generic polyhedra $P(\underline{R}_{\{100\}}; \underline{R}_{\{111\}})$, denoted *cubo-octahedral*, represent intersections of two generic polyhedra, cubic $P(\underline{R}_{\{100\}})$ and octahedral $P(\underline{R}_{\{111\}})$, see figure 6. If the corners of the cubic polyhedron $P(\underline{R}_{\{100\}})$ lie inside the octahedral polyhedron $P(\underline{R}_{\{111\}})$, the resulting combination $P(\underline{R}_{\{100\}}; \underline{R}_{\{111\}})$ will be generic cubic. This requires

$$s_{111}(R_{100}) \leq s_{111}(R_{111}). \quad (44)$$

and according to (7c) and (19c)

$$R_{111} \geq \sqrt{3} R_{100}. \quad (45)$$

On the other hand, if the corners of the octahedral polyhedron $P(\underline{R}_{\{111\}})$ lie inside the cubic polyhedron $P(\underline{R}_{\{100\}})$, the resulting combination $P(\underline{R}_{\{100\}}; \underline{R}_{\{111\}})$ will be generic octahedral. This requires

$$s_{100}(R_{111}) \leq s_{100}(R_{100}) \quad (46)$$

and according to (7a) and (19a)

$$R_{111} \leq 1/\sqrt{3} R_{100}. \quad (47)$$

Thus, the two generic polyhedra intersect and yield a true non-generic polyhedron $P(\underline{R}_{\{100\}}; \underline{R}_{\{111\}})$ with both {100} and {111} facets only for facet distances R_{100}, R_{111} with

$$1/\sqrt{3} R_{100} < R_{111} < \sqrt{3} R_{100} \quad (48)$$

while $P(\underline{R}_{\{100\}}; \underline{R}_{\{111\}})$ is generic cubic for $R_{111} \geq \sqrt{3} R_{100}$ and generic octahedral for $R_{111} \leq 1/\sqrt{3} R_{100}$. As a consequence, generic polyhedra $P(\underline{R}_{\{100\}})$ and $P(\underline{R}_{\{111\}})$ can be described alternatively by non-generic $P(\underline{R}_{\{100\}}; \underline{R}_{\{111\}})$ where

$$P(\underline{R}_{\{100\}}) = P(\underline{R}_{\{100\}}; \underline{R}_{\{111\}}) \quad \text{with } R_{111} \geq \sqrt{3} R_{100} \quad (\text{cubic}) \quad (49a)$$

$$P(\underline{R}_{\{111\}}) = P(\underline{R}_{\{100\}}; \underline{R}_{\{111\}}) \quad \text{with } R_{100} \geq \sqrt{3} R_{111} \quad (\text{octahedral}). \quad (49b)$$

The surfaces of general cubo-octahedral polyhedra $P(\underline{R}_{\{100\}}; \underline{R}_{\{111\}})$ exhibit 6 {100} facets and 8 {111} facets as shown in figure 6. Amongst the intersecting species according to (48) we can distinguish between *truncated octahedral* and *truncated cubic* with *cuboctahedral* polyhedra bridging where

$$1/\sqrt{3} R_{100} < R_{111} < 2/\sqrt{3} R_{100} \quad (\text{truncated octahedral}) \quad (50a)$$

$$2/\sqrt{3} R_{100} < R_{111} < \sqrt{3} R_{100} \quad (\text{truncated cubic}) \quad (50b)$$

$$R_{111} = 2/\sqrt{3} R_{100} \quad (\text{cuboctahedral}) \quad (50c)$$

The surfaces of **truncated octahedral** polyhedra $P(\underline{R}_{\{100\}}; \underline{R}_{\{111\}})$ with $1 < \sqrt{3} R_{111}/R_{100} < 2$ exhibit 6 {100} facets and 8 {111} facets as shown in figure 6(a) and there are 24 polyhedral corners which can be evaluated by methods described in section S.3 of the supplement. They are described by vectors $\underline{C}_{\{1h0\}}$ relative to the center, where in Cartesian coordinates

$$\begin{aligned} \underline{C}_{\{1h0\}} &= R_{100} (\pm 1, \pm h, 0), = R_{100} (\pm h, 0, \pm 1), \\ &= R_{100} (0, \pm 1, \pm h), = R_{100} (\pm 1, 0, \pm h), \\ &= R_{100} (0, \pm h, \pm 1), = R_{100} (\pm h, \pm 1, 0) \\ h &= \sqrt{3} R_{111}/R_{100} - 1, \quad 0 \leq h \leq 1. \end{aligned} \quad (51)$$

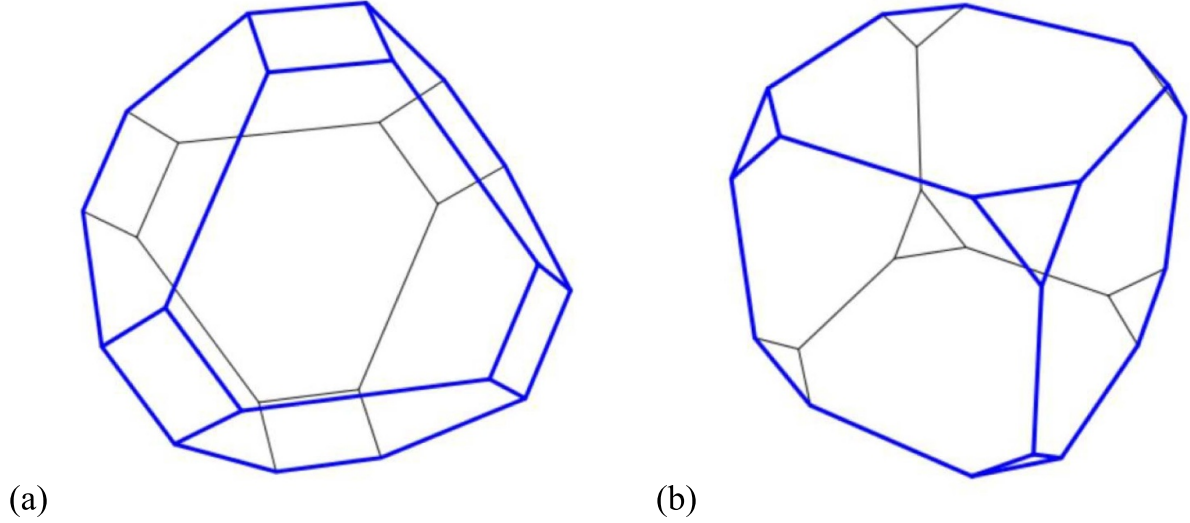


Figure 6. Sketch of cubo-octahedral polyhedra $P(\underline{R}_{\{100\}}; \underline{R}_{\{111\}})$ with front facets in blue and back facets in black, (a) truncated octahedral, $R_{111}/R_{100} = 0.770$, (b) truncated cubic type, $R_{111}/R_{100} = 1.501$.

The 6 $\{100\}$ facets are of the same square shape where each facet extends between four adjacent corners $\underline{C}_{\{1h0\}}$, such as $\underline{C}_{(1h0)}$, $\underline{C}_{(10h)}$, $\underline{C}_{(1-h0)}$, $\underline{C}_{(10-h)}$. The resulting four edges connect corners, such as $\underline{C}_{(1h0)}$ with $\underline{C}_{(10h)}$, at distances d_{f1} given by

$$d_{f1} = \sqrt{2} \left(\sqrt{3}R_{111} - R_{100} \right). \quad (52)$$

The 8 $\{111\}$ facets are of the same hexagonal shape where each facet extends between adjacent corners $\underline{C}_{\{1h0\}}$ and $\underline{C}_{\{111\}}$, such as $\underline{C}_{(1h0)}$, $\underline{C}_{(h10)}$, $\underline{C}_{(01h)}$, $\underline{C}_{(0h1)}$, $\underline{C}_{(h01)}$, $\underline{C}_{(10h)}$. Of the resulting six alternating edges three connect corners, such as $\underline{C}_{(1h0)}$ with $\underline{C}_{(10h)}$, at distances d_{f1} according to (52) while three connect corners, such as $\underline{C}_{(1h0)}$ with $\underline{C}_{(h10)}$, at distances d_{f2} given by

$$d_{f2} = \sqrt{2} \left(2R_{100} - \sqrt{3}R_{111} \right). \quad (53)$$

For $h = 1/2$ all 6 edge lengths are equal leading to regular hexagonal $\{111\}$ facets. As a result, the polyhedron is reminiscent of the shape of Wigner–Seitz cells of bcc crystals [37].

The largest distance from the polyhedral center to its surface along (a, b, c) directions, $s_{abc}(R_{100}, R_{111})$, is given by

$$s_{100}(R_{100}, R_{111}) = R_{100} \quad (54a)$$

$$s_{110}(R_{100}, R_{111}) = \sqrt{3/2} R_{111} \quad (54b)$$

$$s_{111}(R_{100}, R_{111}) = R_{111}. \quad (54c)$$

Further, the area of each square $\{100\}$ facet is given by F_0 where with (52)

$$F_0 = 2 \left(\sqrt{3}R_{111} - R_{100} \right)^2 \quad (55)$$

and of each hexagonal $\{111\}$ facet by F_1 where with (52)

$$F_1 = (3/2)\sqrt{3} \left[R_{111}^2 - \left(\sqrt{3}R_{111} - R_{100} \right)^2 \right]. \quad (56)$$

This yields the total facet surface, F_{surf} (sum over all facet areas) and the volume V_{tot} of the polyhedron according to

$$F_{\text{surf}} = 6F_0 + 8F_1 \quad (57)$$

$$V_{\text{tot}} = (6F_0R_{100} + 8F_1R_{111})/3. \quad (58)$$

The surfaces of **truncated cubic** polyhedra $P(\underline{R}_{\{100\}}; \underline{R}_{\{111\}})$ with $2 < \sqrt{3}R_{111}/R_{100} < 3$ exhibit also 6 $\{100\}$ facets and 8 $\{111\}$ facets as shown in figure 6(b) and there are 24 polyhedral corners which can be evaluated by methods described in section S.3 of the supplement. They are described by vectors $\underline{C}_{\{11g\}}$ relative to the center, where in Cartesian coordinates with (51)

$$\begin{aligned} \underline{C}_{\{11g\}} &= R_{100} (\pm 1, \pm 1, \pm g), = R_{100} (\pm 1, \pm g, \pm 1), \\ &= R_{100} (\pm g, \pm 1, \pm 1) \\ g &= \sqrt{3}R_{111}/R_{100} - 2 = h - 1, \quad 0 \leq g \leq 1. \end{aligned} \quad (59)$$

The 6 $\{100\}$ facets are of the same octagonal shape where each facet extends between eight adjacent corners $\underline{C}_{\{11g\}}$, such as $\underline{C}_{(11g)}$, $\underline{C}_{(1g1)}$, $\underline{C}_{(1-g1)}$, $\underline{C}_{(1-1g)}$, $\underline{C}_{(1-g-1)}$, $\underline{C}_{(1g-1)}$, $\underline{C}_{(11-g)}$. Of the resulting eight alternating edges four connect corners, such as $\underline{C}_{(11g)}$ with $\underline{C}_{(11-g)}$, at distances d_{f3} while four connect corners, such as $\underline{C}_{(11g)}$ with $\underline{C}_{(1g1)}$, at distances d_{f4} given by

$$d_{f3} = \left(2\sqrt{3}R_{111} - 4R_{100} \right) \quad (60)$$

$$d_{f4} = \sqrt{2} \left(3R_{100} - \sqrt{3}R_{111} \right). \quad (61)$$

The 8 $\{111\}$ facets are of the same equilateral triangular shape where each facet extends between three adjacent $\underline{C}_{\{11g\}}$ corners, such as $\underline{C}_{(11g)}$, $\underline{C}_{(g11)}$, $\underline{C}_{(1g1)}$. The resulting three edges connect corners, such as $\underline{C}_{(11g)}$ with $\underline{C}_{(g11)}$, at distances d_{f4} according to (61).

The largest distance from the polyhedral center to its surface along (a, b, c) directions, $s_{abc}(R_{100}, R_{111})$, is given by

$$s_{100}(R_{100}, R_{111}) = R_{100} \quad (62a)$$

$$s_{110}(R_{100}, R_{111}) = \sqrt{2}R_{100} \quad (62b)$$

$$s_{111}(R_{100}, R_{111}) = R_{111}. \quad (62c)$$

Further, the area of each octagonal $\{100\}$ facet is given by F_0 where with (51), (60) and (61)

$$F_0 = 4R_{100}^2 - 2 \left(3R_{100} - \sqrt{3}R_{111} \right)^2 \quad (63)$$

and of each triangular $\{111\}$ facet by F_1 where with (61)

$$F_1 = \sqrt{3} \left(3R_{100} - \sqrt{3}R_{111} \right)^2 / 2. \quad (64)$$

This yields the total facet surface, F_{surf} (sum over all facet areas) and the volume V_{tot} of the polyhedron according to

$$F_{\text{surf}} = 6F_0 + 8F_1 \quad (65)$$

$$V_{\text{tot}} = (6F_0R_{100} + 8F_1R_{111})/3. \quad (66)$$

There are polyhedra which can be assigned to both truncated cubic and truncated octahedral type, the *cuboctahedral* polyhedra $P(\underline{R}_{\{100\}}; \underline{R}_{\{111\}})$ with $\sqrt{3}R_{111}/R_{100} = 2$.

These polyhedra exhibit also 6 $\{100\}$ and 8 $\{111\}$ facets as shown in figure 7 and there are 12 polyhedral corners which can be evaluated by methods described in section S.3 of the supplement. They are described by vectors $\underline{C}_{\{110\}}$ relative to the center, where in Cartesian coordinates

$$\begin{aligned} \underline{C}_{\{110\}} &= R_{100} (\pm 1, \pm 1, 0), = R_{100} (\pm 1, 0, \pm 1), \\ &= R_{100} (0, \pm 1, \pm 1) \end{aligned} \quad (67)$$

which can also be derived from (51) with $h = 1$ or from (59) with $g = 0$.

The 6 $\{100\}$ facets are of the same square shape where each facet extends between four adjacent corners $\underline{C}_{\{110\}}$, such as $\underline{C}_{(110)}$, $\underline{C}_{(101)}$, $\underline{C}_{(1-10)}$, $\underline{C}_{(10-1)}$. The resulting four edges connect corners, such as $\underline{C}_{(110)}$ with $\underline{C}_{(101)}$, at distances d_{f5} derived from (61) and given by

$$d_{f5} = \sqrt{2}R_{100}. \quad (68)$$

The 8 $\{111\}$ facets are of the same equilateral triangular shape where each facet extends between adjacent corners $\underline{C}_{\{110\}}$, such as $\underline{C}_{(110)}$, $\underline{C}_{(011)}$, $\underline{C}_{(101)}$. The resulting three edges connect corners, such as $\underline{C}_{(110)}$ with $\underline{C}_{(101)}$, at distances d_{f5} according to (68).

The largest distance from the polyhedral center to its surface along (a, b, c) directions, $s_{abc}(R_{100}, R_{111})$, is given by

$$s_{100}(R_{100}, R_{111}) = R_{100} \quad (69a)$$

$$s_{110}(R_{100}, R_{111}) = \sqrt{(3/2)} R_{111} = \sqrt{2}R_{100} \quad (69b)$$

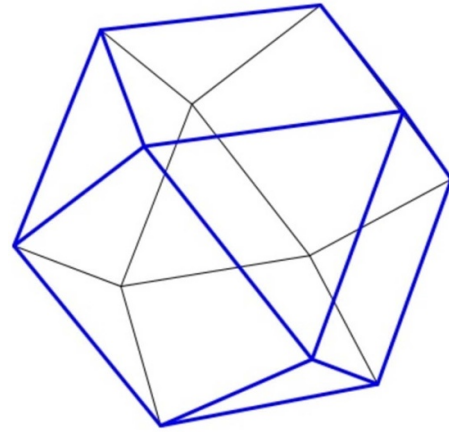


Figure 7. Sketch of cuboctahedral polyhedron $P(\underline{R}_{\{100\}}; \underline{R}_{\{111\}})$ where $R_{111}/R_{100} = 1.155$ with front facets in blue and back facets in black.

$$s_{111}(R_{100}, R_{111}) = R_{111} = (2/\sqrt{3})R_{100}. \quad (69c)$$

Further, the area of each square $\{100\}$ facet is given by F_0 where with (68)

$$F_0 = 2R_{100}^2 \quad (70)$$

and of each hexagonal $\{111\}$ facet by F_1 where with (68)

$$F_1 = (\sqrt{3})/2 R_{100}^2. \quad (71)$$

Thus, the total facet surface, F_{surf} (sum over all facet areas) and the volume V_{tot} of the polyhedron are given by

$$F_{\text{surf}} = 6F_0 + 8F_1 = 4 \left(3 + \sqrt{3} \right) R_{100}^2 \quad (72)$$

$$V_{\text{tot}} = \left(6F_0R_{100} + 8F_1 \left(2/\sqrt{3}R_{100} \right) \right) / 3 = (20/3)R_{100}^3. \quad (73)$$

3.2.3. Rhombo-octahedral polyhedra $P(\underline{R}_{\{110\}}; \underline{R}_{\{111\}})$. Non-generic polyhedra $P(\underline{R}_{\{110\}}; \underline{R}_{\{111\}})$, denoted *rhombo-octahedral*, represent intersections of two generic polyhedra, rhombohedral $P(\underline{R}_{\{110\}})$ and octahedral $P(\underline{R}_{\{111\}})$, see figure 8. If the edges of the rhombohedral polyhedron $P(\underline{R}_{\{110\}})$ lie inside the octahedral polyhedron $P(\underline{R}_{\{111\}})$, the resulting combination $P(\underline{R}_{\{110\}}; \underline{R}_{\{111\}})$ will be generic rhombohedral. This requires

$$s_{111}(R_{110}) \leq s_{111}(R_{111}). \quad (74)$$

and according to (13c) and (19c)

$$R_{111} \geq \sqrt{(3/2)}R_{110}. \quad (75)$$

On the other hand, if the corners of the octahedral polyhedron $P(\underline{R}_{\{111\}})$ lie inside the rhombohedral polyhedron

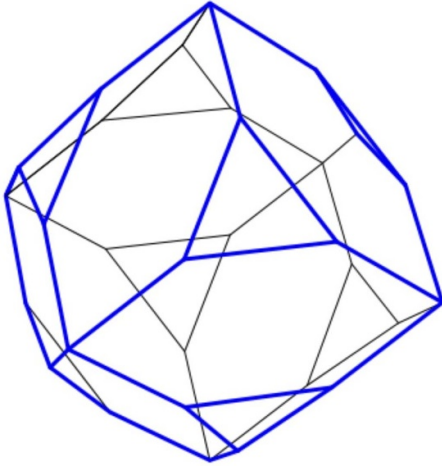


Figure 8. Sketch of rhombo-octahedral polyhedron $P(\underline{R}_{\{110\}}; \underline{R}_{\{111\}})$, $R_{110}/R_{111} = 0.942$, with front facets in blue and back facets in black.

$P(\underline{R}_{\{110\}})$, the resulting combination $P(\underline{R}_{\{110\}}; \underline{R}_{\{111\}})$ will be generic octahedral. This requires

$$s_{100}(R_{111}) \leq s_{100}(R_{110}) \quad (76)$$

and according to (13a) and (19a)

$$R_{111} \leq \sqrt[3]{(2/3)R_{110}}. \quad (77)$$

Thus, the two generic polyhedra intersect and yield a true non-generic polyhedron $P(\underline{R}_{\{110\}}; \underline{R}_{\{111\}})$ with both $\{110\}$ and $\{111\}$ facets only for facet distances R_{110}, R_{111} with

$$\sqrt[3]{(2/3)R_{110}} < R_{111} < \sqrt[3]{(3/2)R_{110}} \quad (78)$$

while $P(\underline{R}_{\{110\}}; \underline{R}_{\{111\}})$ is generic rhombohedral for $R_{111} \geq \sqrt[3]{(3/2)R_{110}}$ and generic octahedral for $R_{111} \leq \sqrt[3]{(2/3)R_{110}}$. As a consequence, generic polyhedra $P(\underline{R}_{\{110\}})$ and $P(\underline{R}_{\{111\}})$ can be described alternatively by non-generic $P(\underline{R}_{\{110\}}; \underline{R}_{\{111\}})$ where

$$P(\underline{R}_{\{110\}}) = P(\underline{R}_{\{110\}}; \underline{R}_{\{111\}}) \text{ with } R_{111} \geq \sqrt[3]{(3/2)R_{110}} \quad (\text{rhombohedral}) \quad (79a)$$

$$P(\underline{R}_{\{111\}}) = P(\underline{R}_{\{110\}}; \underline{R}_{\{111\}}) \text{ with } R_{110} \geq \sqrt[3]{(3/2)R_{111}} \quad (\text{octahedral}). \quad (79b)$$

The surfaces of general rhombo-octahedral polyhedra $P(\underline{R}_{\{110\}}; \underline{R}_{\{111\}})$ exhibit 12 $\{110\}$ facets and 8 $\{111\}$ facets as shown in figure 8.

There are 30 polyhedral corners which can be evaluated by methods described in section S.3 of the supplement. They fall into two groups of 6 and 24 corners each, described by vectors $\underline{C}_{\{100\}}$ and $\underline{C}_{\{1hh\}}$ relative to the center, where in Cartesian coordinates

$$\begin{aligned} \underline{C}_{\{100\}} &= \sqrt{2}R_{110}(\pm 1, 0, 0), = \sqrt{2}R_{110}(0, \pm 1, 0), \\ &= \sqrt{2}R_{110}(0, 0, \pm 1) \\ \underline{C}_{\{1hh\}} &= R(\pm 1, \pm h, \pm h), = R(\pm h, \pm 1, \pm h), \\ &= R(\pm h, \pm h, \pm 1) \\ R &= 2\sqrt{2}R_{110} - \sqrt{3}R_{111}, h = (\sqrt{3}R_{111} - \sqrt{2}R_{110})/R, 0 \leq h \leq 1. \end{aligned} \quad (80)$$

The 12 $\{110\}$ facets are of the same hexagonal shape where each facet extends between six adjacent corners $\underline{C}_{\{100\}}$ and $\underline{C}_{\{1hh\}}$, such as $\underline{C}_{\{100\}}$, $\underline{C}_{\{1hh\}}$, $\underline{C}_{\{hh1\}}$, $\underline{C}_{\{001\}}$, $\underline{C}_{\{h-h1\}}$, $\underline{C}_{\{1-hh\}}$. Of the resulting six edges two connect corners, such as $\underline{C}_{\{1hh\}}$ with $\underline{C}_{\{hh1\}}$, at distances d_{g1} while four connect corners, such as $\underline{C}_{\{100\}}$ with $\underline{C}_{\{1hh\}}$, at distances d_{g2} given by

$$d_{g1} = \sqrt{2} \left(3\sqrt{2}R_{110} - 2\sqrt{3}R_{111} \right) \quad (81)$$

$$d_{g2} = \sqrt{3} \left(\sqrt{3}R_{111} - \sqrt{2}R_{110} \right). \quad (82)$$

The 8 triangular $\{111\}$ facets are of the same equilateral triangular shape where each facet extends between adjacent corners $\underline{C}_{\{1hh\}}$, such as $\underline{C}_{\{1hh\}}$, $\underline{C}_{\{h1h\}}$, $\underline{C}_{\{hh1\}}$. The resulting three edges connect corners, such as $\underline{C}_{\{1hh\}}$ with $\underline{C}_{\{hh1\}}$, at distances d_{g1} according to (81).

The largest distance from the polyhedral center to its surface along (a, b, c) directions, $s_{abc}(R_{110}, R_{111})$, is given by

$$s_{100}(R_{110}, R_{111}) = \sqrt{2}R_{110} \quad (83a)$$

$$s_{110}(R_{110}, R_{111}) = R_{110} \quad (83b)$$

$$s_{111}(R_{110}, R_{111}) = R_{111}. \quad (83c)$$

Further, the area of each hexagonal $\{110\}$ facet is given by F_0 where with (80)

$$F_0 = 2\sqrt{2} \left(\sqrt{3}R_{111} - \sqrt{2}R_{110} \right) \left(2\sqrt{2}R_{110} - \sqrt{3}R_{111} \right) \quad (84)$$

and of each triangular $\{111\}$ facet by F_1 where with (81)

$$F_1 = \sqrt{3/4} \left(3\sqrt{2}R_{110} - 2\sqrt{3}R_{111} \right)^2 \quad (85)$$

This yields the total facet surface, F_{surf} (sum over all facet areas) and the volume V_{tot} of the polyhedron according to

$$F_{\text{surf}} = 12F_0 + 8F_1 \quad (86)$$

$$V_{\text{tot}} = (12F_0R_{110} + 8F_1R_{111})/3. \quad (87)$$

3.2.4. Cubo-rhombic polyhedra

$P(\underline{R}_{\{100\}}; \underline{R}_{\{110\}}; \underline{R}_{\{111\}})$. Non-generic polyhedra $P(\underline{R}_{\{100\}}; \underline{R}_{\{110\}}; \underline{R}_{\{111\}})$, denoted *cubo-rhombic*, represent intersections of three generic polyhedra, cubic $P(\underline{R}_{\{100\}})$, rhombohedral $P(\underline{R}_{\{110\}})$, and octahedral $P(\underline{R}_{\{111\}})$. Thus, they show in the most general case $\{100\}$, $\{110\}$, and $\{111\}$ facets. A full discussion of these polyhedra requires results for generic and non-generic polyhedra, see sections 3.1 and 3.2.1–3, as will be detailed in the following.

First, we consider the general notation for generic polyhedra discussed in section 3.1. Cubic polyhedra $P(\underline{R}_{\{100\}})$ lie completely inside rhombohedral polyhedra $P(\underline{R}_{\{110\}})$ if $R_{110} \geq \sqrt{2} R_{100}$ according to (31) and inside octahedral polyhedra $P(\underline{R}_{\{111\}})$ if $R_{111} \geq \sqrt{3} R_{100}$ according to (45). This leads to polyhedra $P(\underline{R}_{\{100\}}; \underline{R}_{\{110\}}; \underline{R}_{\{111\}})$ which are generic cubic where

$$P(\underline{R}_{\{100\}}; \underline{R}_{\{110\}}; \underline{R}_{\{111\}}) = P(\underline{R}_{\{100\}}) \text{ if } R_{100} \leq \min(1/\sqrt{2} R_{110}, 1/\sqrt{3} R_{111}). \quad (88)$$

The two constraints on R_{100} can also be interpreted as cubic $P(\underline{R}_{\{100\}})$ lying completely inside rhombo-octahedral $P(\underline{R}_{\{110\}}; \underline{R}_{\{111\}})$.

Rhombohedral polyhedra $P(\underline{R}_{\{110\}})$ lie completely inside cubic polyhedra $P(\underline{R}_{\{100\}})$ if $R_{100} \geq \sqrt{2} R_{110}$ according to (32) and inside octahedral polyhedra $P(\underline{R}_{\{111\}})$ if $R_{111} \geq \sqrt{(3/2)} R_{110}$ according to (75). This leads to polyhedra $P(\underline{R}_{\{100\}}; \underline{R}_{\{110\}}; \underline{R}_{\{111\}})$ which are generic rhombohedral where

$$P(\underline{R}_{\{100\}}; \underline{R}_{\{110\}}; \underline{R}_{\{111\}}) = P(\underline{R}_{\{110\}}) \text{ if } R_{110} \leq \min(1/\sqrt{2} R_{100}, \sqrt{(2/3)} R_{111}). \quad (89)$$

The two constraints on R_{110} can also be interpreted as rhombohedral $P(\underline{R}_{\{110\}})$ lying completely inside cubo-octahedral $P(\underline{R}_{\{100\}}; \underline{R}_{\{111\}})$.

Octahedral polyhedra $P(\underline{R}_{\{111\}})$ lie completely inside cubic polyhedra $P(\underline{R}_{\{100\}})$ if $R_{100} \geq \sqrt{3} R_{111}$ according to (47) and inside rhombohedral polyhedra $P(\underline{R}_{\{110\}})$ if $R_{110} \geq \sqrt{(3/2)} R_{111}$ according to (77). This leads to polyhedra $P(\underline{R}_{\{100\}}; \underline{R}_{\{110\}}; \underline{R}_{\{111\}})$ which are generic octahedral where

$$P(\underline{R}_{\{100\}}; \underline{R}_{\{110\}}; \underline{R}_{\{111\}}) = P(\underline{R}_{\{111\}}) \text{ if } R_{111} \leq \min(1/\sqrt{3} R_{100}, \sqrt{(2/3)} R_{110}). \quad (90)$$

The two constraints on R_{111} can also be interpreted as octahedral $P(\underline{R}_{\{111\}})$ lying completely inside cubo-rhombic $P(\underline{R}_{\{100\}}; \underline{R}_{\{110\}})$.

General notations of non-generic polyhedra with two facet types, discussed in sections 3.2.1–3, are obtained by analogous arguments combining the previous constraints. True cubo-rhombic polyhedra $P(\underline{R}_{\{100\}}; \underline{R}_{\{110\}})$ with (34) lie completely

inside octahedral polyhedra $P(\underline{R}_{\{111\}})$ if $R_{111} \geq \sqrt{3} R_{100}$ according to (45) and if $R_{111} \geq \sqrt{(3/2)} R_{110}$ according to (75). Thus,

$$P(\underline{R}_{\{100\}}; \underline{R}_{\{110\}}; \underline{R}_{\{111\}}) = P(\underline{R}_{\{100\}}; \underline{R}_{\{110\}}) \text{ if } R_{111} \geq \min(\sqrt{3} R_{100}, \sqrt{(3/2)} R_{110}) \quad (91)$$

yielding with (34)

$$R_{111} \geq \sqrt{(3/2)} R_{110}. \quad (92)$$

True cubo-octahedral polyhedra $P(\underline{R}_{\{100\}}; \underline{R}_{\{111\}})$ with (48) lie completely inside rhombohedral polyhedra $P(\underline{R}_{\{110\}})$ if $R_{110} \geq \sqrt{2} R_{100}$ according to (31) and if $R_{110} \geq \sqrt{(3/2)} R_{111}$ according to (77). Thus,

$$P(\underline{R}_{\{100\}}; \underline{R}_{\{110\}}; \underline{R}_{\{111\}}) = P(\underline{R}_{\{100\}}; \underline{R}_{\{111\}}) \text{ if } R_{110} \geq \min(\sqrt{2} R_{100}, \sqrt{(3/2)} R_{111}) \quad (93)$$

yielding with (50a)–(50c)

$$R_{110} \geq \sqrt{(3/2)} R_{111} \text{ for } P(\underline{R}_{\{100\}}; \underline{R}_{\{111\}}) \text{ of truncated octahedral type} \quad (94a)$$

$$R_{110} \geq \sqrt{2} R_{100} \text{ for } P(\underline{R}_{\{100\}}; \underline{R}_{\{111\}}) \text{ of truncated cubic type} \quad (94b)$$

$$R_{110} = \sqrt{2} R_{100} = \sqrt{(3/2)} R_{111} \text{ for } P(\underline{R}_{\{100\}}; \underline{R}_{\{111\}}) \text{ of cuboctahedral type} \quad (94c)$$

True rhombo-octahedral polyhedra $P(\underline{R}_{\{110\}}; \underline{R}_{\{111\}})$ with (78) lie completely inside cubic polyhedra $P(\underline{R}_{\{100\}})$ if $R_{100} \geq \sqrt{2} R_{110}$ according to (32) and if $R_{100} \geq \sqrt{3} R_{111}$ according to (47). Thus,

$$P(\underline{R}_{\{100\}}; \underline{R}_{\{110\}}; \underline{R}_{\{111\}}) = P(\underline{R}_{\{110\}}; \underline{R}_{\{111\}}) \text{ if } R_{100} \geq \min(\sqrt{2} R_{110}, \sqrt{3} R_{111}) \quad (95)$$

yielding with (78)

$$R_{100} \geq \sqrt{2} R_{110}. \quad (96)$$

The above constraints on R_{abc} can be rephrased to treat the most general case of true cubo-rhombic polyhedra $P(\underline{R}_{\{100\}}; \underline{R}_{\{110\}}; \underline{R}_{\{111\}})$ which exhibit $\{100\}$, $\{110\}$, as well as $\{111\}$ facets. According to (34), true cubo-rhombic $P(\underline{R}_{\{100\}}; \underline{R}_{\{110\}})$ appear for

$$1/\sqrt{2} R_{110} < R_{100} < \sqrt{2} R_{110}. \quad (97)$$

Intersecting $P(\underline{R}_{\{100\}}; \underline{R}_{\{110\}})$ with $P(\underline{R}_{\{111\}})$ to yield a true non-generic polyhedron $P(\underline{R}_{\{100\}}; \underline{R}_{\{110\}}; \underline{R}_{\{111\}})$ requires according to (91) and (90)

$$\sqrt[3]{(2/3) R_{111}} < R_{110} < \sqrt[3]{(3/2) R_{111}} \quad (98)$$

$$1/\sqrt[3]{3} R_{100} < R_{111} < \sqrt[3]{3} R_{100}. \quad (99)$$

Altogether, true non-generic polyhedra $P(\underline{R}_{\{100\}}; \underline{R}_{\{110\}}; \underline{R}_{\{111\}})$ appear if constraints (97)–(99) are fulfilled.

Intersecting $P(\underline{R}_{\{100\}}; \underline{R}_{\{111\}})$ with $P(\underline{R}_{\{110\}})$ to yield a true non-generic polyhedron $P(\underline{R}_{\{100\}}; \underline{R}_{\{110\}}; \underline{R}_{\{111\}})$ is found to yield constraints on the facet distances R_{abc} which are identical with (97)–(99). This applies also to intersecting $P(\underline{R}_{\{110\}}; \underline{R}_{\{111\}})$ with $P(\underline{R}_{\{100\}})$. Thus, a complete analysis of the structure of true cubo-rhombic polyhedra $P(\underline{R}_{\{100\}}; \underline{R}_{\{110\}}; \underline{R}_{\{111\}})$ can be achieved by considering only one scenario where, in the following, we focus on intersecting cubo-rhombic $P(\underline{R}_{\{100\}}; \underline{R}_{\{110\}})$ with octahedral $P(\underline{R}_{\{111\}})$.

3.2.4.1. Polyhedra $P(\underline{R}_{\{100\}}; \underline{R}_{\{110\}}; \underline{R}_{\{111\}})$ by intersection.

Intersecting cubo-rhombic $P(\underline{R}_{\{100\}}; \underline{R}_{\{110\}})$ with octahedral $P(\underline{R}_{\{111\}})$ polyhedra results in different polyhedral shapes depending on the relative sizes of the corresponding facet distances R_{abc} . Fixing R_{100} and R_{110} with (97) the shape of $P(\underline{R}_{\{100\}}; \underline{R}_{\{110\}}; \underline{R}_{\{111\}})$ is fully determined by the size of its facet distance R_{111} . According to (97), (98) and (90) R_{111} must always be within the range

$$1/\sqrt[3]{3} R_{100} \leq R_{111} \leq \sqrt[3]{(3/2) R_{110}} \quad (100)$$

where there are two regions leading to different polyhedral shape,

$$\begin{aligned} \text{outer region : } R_{111}^s &\leq R_{111} \leq \sqrt[3]{(3/2) R_{110}} \text{ with} \\ R_{111}^s &= 1/\sqrt[3]{3} (2\sqrt[3]{2} R_{110} - R_{100}) \end{aligned} \quad (101)$$

$$\begin{aligned} \text{inner region : } R_{111}^b &\leq R_{111} \leq R_{111}^s \text{ with} \\ R_{111}^b &= \sqrt[3]{(2/3) R_{110}} \end{aligned} \quad (102)$$

as illustrated in figure 9 by a cubo-rhombic polyhedron $P(\underline{R}_{\{100\}}; \underline{R}_{\{110\}})$ where the dashed red triangle shows a cut along $\{111\}$ indicating the boundary between the outer and inner region of corresponding cubo-rhombic polyhedra $P(\underline{R}_{\{100\}}; \underline{R}_{\{110\}}; \underline{R}_{\{111\}})$.

The **outer region** is determined by R_{111} values with $R_{111}^s \leq R_{111} \leq \sqrt[3]{(3/2) R_{110}}$ according to (101). Here the initial polyhedron $P(\underline{R}_{\{100\}}; \underline{R}_{\{110\}})$ is capped at its corners $\underline{C}_{\{111\}}$ forming $\{111\}$ facets. This results in 6 $\{100\}$, 12 $\{110\}$, and 8 $\{111\}$ facets as shown in figure 10.

There are 48 polyhedral corners which can be evaluated by methods described in section S.3 of the supplement. They fall into two groups of 24 corners each, described by vectors $\underline{C}_{\{1gg\}}$ and $\underline{C}_{\{1hh\}}$ relative to the center, where in Cartesian coordinates

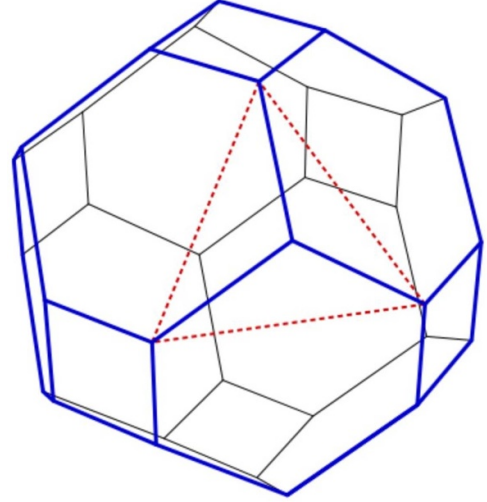


Figure 9. Sketch of cubo-rhombic polyhedron $P(\underline{R}_{\{100\}}; \underline{R}_{\{110\}})$, $R_{110}/R_{100} = 0.884$, $R_{111}/R_{100} = 1.083$, with front facets in blue and back facets in black. The dashed red triangle shows a cut along $\{111\}$ indicating the boundary between the outer and inner region of corresponding cubo-rhombic polyhedra $P(\underline{R}_{\{100\}}; \underline{R}_{\{110\}}; \underline{R}_{\{111\}})$ for $R_{111} = R_{111}^s$, $R_{111}/R_{100} = 0.866$, see text.

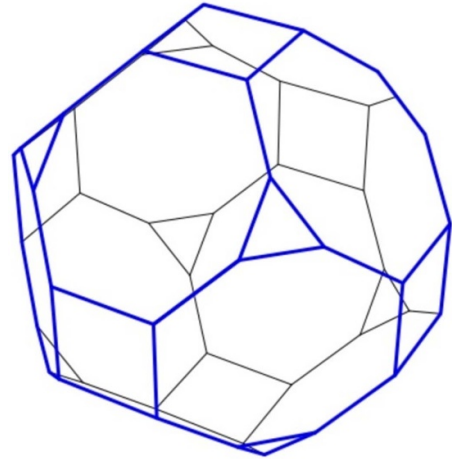


Figure 10. Sketch of cubo-rhombic polyhedron $P(\underline{R}_{\{100\}}; \underline{R}_{\{110\}}; \underline{R}_{\{111\}})$, $R_{110}/R_{100} = 0.884$, $R_{111}/R_{100} = 1.010$, $R_{111} \geq R_{111}^s$ (outer region), see text, with front facets in blue and back facets in black.

$$\begin{aligned} \underline{C}_{\{1gg\}} &= R_{100} (\pm 1, \pm g, \pm g), = R_{100} (\pm g, \pm 1, \pm g), \\ &= R_{100} (\pm g, \pm g, \pm 1), \\ \underline{C}_{\{1hh\}} &= R (\pm 1, \pm h, \pm h), = R (\pm h, \pm 1, \pm h), \\ &= R (\pm h, \pm h, \pm 1) \\ g &= (\sqrt[3]{2} R_{110} - R_{100})/R_{100}, \quad h = (\sqrt[3]{3} R_{111} - \sqrt[3]{2} R_{110})/R \\ 0 \leq g \leq 1, \quad 0 \leq h \leq 1, \quad R &= (2\sqrt[3]{2} R_{110} - \sqrt[3]{3} R_{111}). \end{aligned} \quad (103)$$

The 6 $\{100\}$ facets are of the same square shape where each facet extends between four adjacent corners $\underline{C}_{\{1gg\}}$, such as

$\underline{C}_{\{1gg\}}, \underline{C}_{\{1-gg\}}, \underline{C}_{\{1-g-g\}}, \underline{C}_{\{1g-g\}}$. The resulting four edges connect corners, such as $\underline{C}_{\{1gg\}}$ with $\underline{C}_{\{1-gg\}}$, at distances d_{h1} given by

$$d_{h1} = 2 \left(\sqrt{2}R_{110} - R_{100} \right). \quad (104)$$

The 12 {110} facets are of the same octagonal shape where each facet extends between eight adjacent corners $\underline{C}_{\{1gg\}}$ and $\underline{C}_{\{1hh\}}$, such as $\underline{C}_{\{1gg\}}, \underline{C}_{\{1hh\}}, \underline{C}_{\{hh1\}}, \underline{C}_{\{gg1\}}, \underline{C}_{\{g-g1\}}, \underline{C}_{\{h-h1\}}, \underline{C}_{\{1-hh\}}, \underline{C}_{\{1-gg\}}$. Of the resulting eight edges two connect corners, such as $\underline{C}_{\{1gg\}}$ with $\underline{C}_{\{1-gg\}}$, at distances d_{h1} given by (104) while another two connect corners, such as $\underline{C}_{\{1hh\}}$ to $\underline{C}_{\{hh1\}}$, at distances d_{h2} and four connect corners, such as $\underline{C}_{\{1gg\}}$ with $\underline{C}_{\{1hh\}}$, at distances d_{h3} given by

$$d_{h2} = \sqrt{2} \left(3\sqrt{2}R_{110} - 2\sqrt{3}R_{111} \right) \quad (105)$$

$$d_{h3} = \sqrt{3} \left(R_{100} - 2\sqrt{2}R_{110} + \sqrt{3}R_{111} \right). \quad (106)$$

The 8 {111} facets are of the same equilateral triangular shape where each facet extends between adjacent corners $\underline{C}_{\{1hh\}}$, such as $\underline{C}_{\{1hh\}}, \underline{C}_{\{h1h\}}, \underline{C}_{\{hh1\}}$. The resulting three edges connect corners, such as $\underline{C}_{\{1hh\}}$ with $\underline{C}_{\{hh1\}}$, at distances d_{h2} according to (105).

Clearly, the largest distance from the polyhedral center to its surface along (a, b, c) directions, $s_{abc}(R_{100}, R_{110}, R_{111})$, equals the corresponding facet distance R_{abc} i.e.

$$s_{abc}(R_{100}, R_{110}, R_{111}) = R_{abc}. \quad (107)$$

Further, the area of each square {100} facet is given by F_0 where with (104)

$$F_0 = 4 \left(\sqrt{2}R_{110} - R_{100} \right)^2 \quad (108)$$

and of each octagonal {110} facet by F_1 where with (103)

$$F_1 = 2\sqrt{2} \left[\left(\sqrt{3}R_{111} - \sqrt{2}R_{110} \right) \left(2\sqrt{2}R_{110} - \sqrt{3}R_{111} \right) - \left(\sqrt{2}R_{110} - R_{100} \right)^2 \right] \quad (109)$$

and of each triangular {111} facet by F_2 where with (105)

$$F_2 = \left(\sqrt{3} \right) / 2 \left(3\sqrt{2}R_{110} - 2\sqrt{3}R_{111} \right)^2. \quad (110)$$

This yields the total facet surface, F_{surf} (sum over all facet areas) and the volume V_{tot} of the polyhedron according to

$$F_{\text{surf}} = 6F_0 + 12F_1 + 8F_2 \quad (111)$$

$$V_{\text{tot}} = (6F_0R_{100} + 12F_1R_{110} + 8F_2R_{111})/3. \quad (112)$$

At the bottom of the outer region, i.e. for $R_{111} = R_{111}^s$ according to (101) the polyhedron $P(\underline{R}_{\{100\}}; \underline{R}_{\{110\}}; \underline{R}_{\{111\}})$ assumes a particular shape. As before, there are 6 {100}, 12 {110}, and 8 {111} facets as shown in figures 11(a) and (b).

However, the number of polyhedral corners is reduced to 24 and their Cartesian coordinates are obtained from (103) setting $R_{111} = R_{111}^s$ with (101) which yields

$$R = R_{100}, \quad g = h = \left(\sqrt{2}R_{110} - R_{100} \right) / R_{100} \quad (113)$$

and thus

$$\begin{aligned} \underline{C}_{\{1gg\}} &= R_{100} (\pm 1, \pm g, \pm g), = R_{100} (\pm g, \pm 1, \pm g), \\ &= R_{100} (\pm g, \pm g, \pm 1). \end{aligned} \quad (114)$$

The 6 {100} facets are of the same square shape where each facet extends between four adjacent corners $\underline{C}_{\{1gg\}}$, such as $\underline{C}_{\{1gg\}}, \underline{C}_{\{1-gg\}}, \underline{C}_{\{1-g-g\}}, \underline{C}_{\{1g-g\}}$. The resulting four edges connect corners, such as $\underline{C}_{\{1gg\}}$ with $\underline{C}_{\{1-gg\}}$, at distances d_{h4} given by

$$d_{h4} = 2 \left(\sqrt{2}R_{110} - R_{100} \right). \quad (115)$$

The 12 {110} facets are of the same rectangular shape where each facet extends between four adjacent corners $\underline{C}_{\{1gg\}}$, such as $\underline{C}_{\{1gg\}}, \underline{C}_{\{gg1\}}, \underline{C}_{\{g-g1\}}, \underline{C}_{\{1-gg\}}$. Of the resulting four edges two connect corners, such as $\underline{C}_{\{1gg\}}$ with $\underline{C}_{\{1-gg\}}$, at distances d_{h4} according to (115) while two connect corners, such as $\underline{C}_{\{1gg\}}$ with $\underline{C}_{\{gg1\}}$, at distances d_{h5} given by

$$d_{h5} = \sqrt{2} \left(2R_{100} - \sqrt{2}R_{110} \right). \quad (116)$$

The 8 {111} facets are of the same equilateral triangular shape where each facet extends between adjacent corners $\underline{C}_{\{1gg\}}$, such as $\underline{C}_{\{1gg\}}, \underline{C}_{\{g1g\}}, \underline{C}_{\{gg1\}}$. The resulting three edges connect corners, such as $\underline{C}_{\{1gg\}}$ with $\underline{C}_{\{gg1\}}$, at distances d_{h5} according to (116).

Clearly, the largest distance from the polyhedral center to its surface along (a, b, c) directions, $s_{abc}(R_{100}, R_{110}, R_{111})$, equals the corresponding facet distance R_{abc} i.e.

$$s_{abc}(R_{100}, R_{110}, R_{111}) = R_{abc}. \quad (117)$$

Further, the area of each square {100} facet is given by F_0 where with (115)

$$F_0 = 4 \left(\sqrt{2}R_{110} - R_{100} \right)^2 \quad (118)$$

and of each rectangular {110} facet by F_1 where with (115) and (116)

$$F_1 = 2\sqrt{2} \left(\sqrt{2}R_{110} - R_{100} \right) \left(2R_{100} - \sqrt{2}R_{110} \right) \quad (119)$$

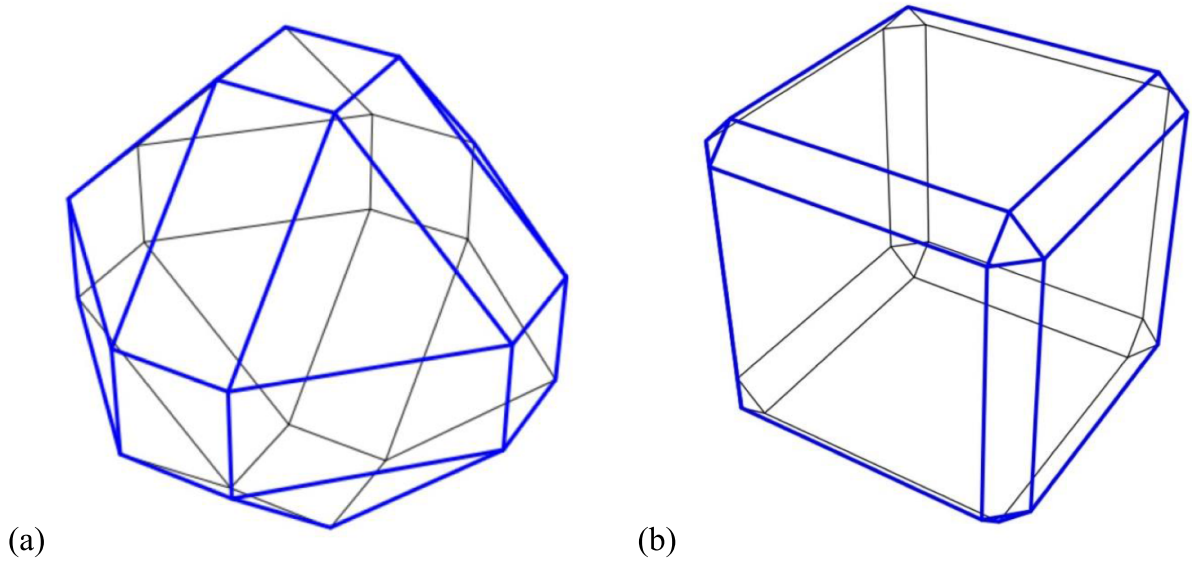


Figure 11. Sketch of cubo-rhombic polyhedron $P(\underline{R}_{\{100\}}; \underline{R}_{\{110\}}; \underline{R}_{\{111\}})$ with (a) $R_{110}/R_{100} = 0.884$, $R_{111}/R_{100} = 0.866$, (b) $R_{110}/R_{100} = 1.282$, $R_{111}/R_{100} = 1.516$, $R_{111} = R_{111}^s$, see text, with front facets in blue and back facets in black.

and of each triangular $\{111\}$ facet by F_2 where with (116)

$$F_2 = (\sqrt{3})/2 (2R_{100} - \sqrt{2}R_{110})^2. \quad (120)$$

This yields the total facet surface, F_{surf} (sum over all facet areas) and the volume V_{tot} of the polyhedron according to

$$F_{\text{surf}} = 6F_0 + 12F_1 + 8F_2 \quad (121)$$

$$V_{\text{tot}} = (6F_0R_{100} + 12F_1R_{110} + 8F_2R_{111})/3. \quad (122)$$

Polyhedra $P(\underline{R}_{\{100\}}; \underline{R}_{\{110\}}; \underline{R}_{\{111\}})$ with $R_{111} = R_{111}^s$ and R_{110} less than but close to $\sqrt{2} R_{100}$ take the shape of cubes whose edges and corners are capped, as shown in figure 11(b), where the capping becomes smaller for R_{110} closer to $\sqrt{2} R_{100}$. These polyhedra can be used to simulate cubic NPs with smooth edges and corners observed in many experiments mentioned in section 3.1.1.

The **inner region** is determined by R_{111} values with $R_{111}^b \leq R_{111} \leq R_{111}^s$ according to (102) and (101). Here the polyhedron $P(\underline{R}_{\{100\}}; \underline{R}_{\{110\}}; \underline{R}_{\{111\}})$ with $R_{111} = R_{111}^s$ is capped further which still results in 6 $\{100\}$, 12 $\{110\}$, and 8 $\{111\}$ facets, however, with changed shapes as shown in figure 12 and discussed below.

There are 48 polyhedral corners which can be evaluated by methods described in section S.3 of the supplement. They are described by vectors $\underline{C}_{\{1gh\}}$ relative to the center, where in Cartesian coordinates

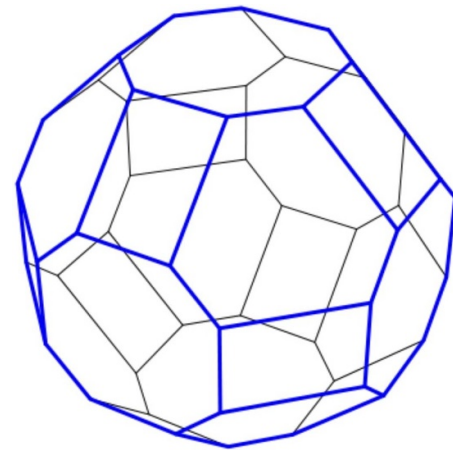


Figure 12. Sketch of cubo-rhombic polyhedron $P(\underline{R}_{\{100\}}; \underline{R}_{\{110\}}; \underline{R}_{\{111\}})$, $R_{110}/R_{100} = 1.061$, $R_{111}/R_{100} = 1.010$, $R_{111}^b \leq R_{111} \leq R_{111}^s$ (inner region), see text, with front facets in blue and back facets in black.

$$\begin{aligned} \underline{C}_{\{1gh\}} &= R_{100} (\pm 1, \pm g, \pm h), = R_{100} (\pm g, \pm 1, \pm h), \\ &= R_{100} (\pm g, \pm h, \pm 1), = R_{100} (\pm 1, \pm h, \pm g), \\ &= R_{100} (\pm h, \pm 1, \pm g), = R_{100} (\pm h, \pm g, \pm 1) \\ g &= (\sqrt{2}R_{110} - R_{100})/R_{100}, h = (\sqrt{3}R_{111} - \sqrt{2}R_{110})/R_{100} \\ 0 \leq g \leq 1, \quad 0 \leq h \leq 1. \end{aligned} \quad (123)$$

The 6 $\{100\}$ facets are of the same octagonal shape where each facet extends between eight adjacent corners $\underline{C}_{\{1gh\}}$, such as $\underline{C}_{(1gh)}$, $\underline{C}_{(1hg)}$, $\underline{C}_{(1-hg)}$, $\underline{C}_{(1-g-h)}$, $\underline{C}_{(1-g-h)}$, $\underline{C}_{(1-h-g)}$, $\underline{C}_{(1h-g)}$, $\underline{C}_{(1g-h)}$. Of the resulting eight alternating edges four connect corners, such as $\underline{C}_{(1gh)}$ with $\underline{C}_{(1g-h)}$, at distances d_{h6} while four connect corners, such as $\underline{C}_{(1gh)}$ with $\underline{C}_{(1hg)}$, at distances d_{h7} given by

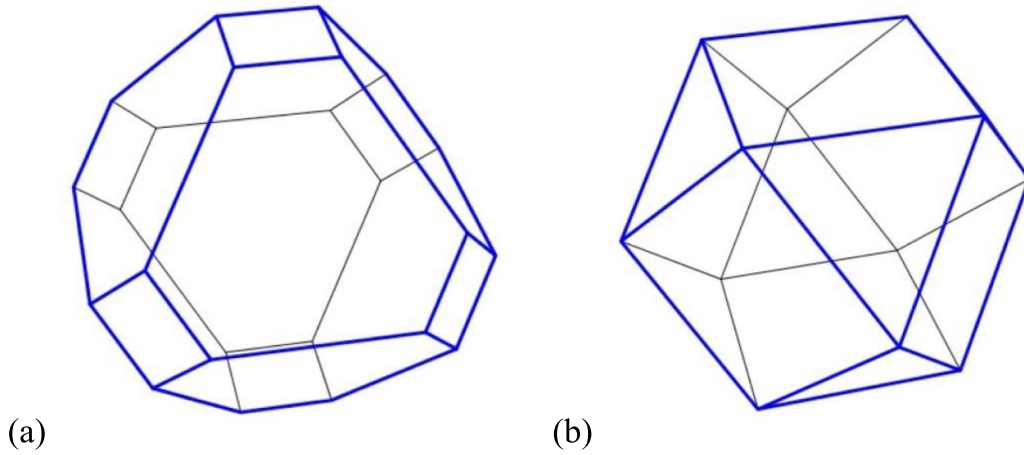


Figure 13. Sketch of cubo-rhomb-octahedral polyhedra $P(\underline{R}_{\{100\}}; \underline{R}_{\{110\}}; \underline{R}_{\{111\}})$ with $R_{111} = R_{111}^b$, see text. (a) $R_{110}/R_{100} = 0.943$, $R_{111}/R_{100} = 0.770$, cubo-octahedral (truncated octahedral); (b) $R_{110}/R_{100} = 1.414$, $R_{111}/R_{100} = 1.155$, cuboctahedral. Front facets are shown in blue and back facets in black.

$$d_{h6} = 2 \left(\sqrt{3} R_{111} - \sqrt{2} R_{110} \right) \quad (124)$$

$$d_{h7} = \sqrt{2} \left(2\sqrt{2} R_{110} - R_{100} - \sqrt{3} R_{111} \right). \quad (125)$$

The 12 $\{110\}$ facets are of the same rectangular shape where each facet extends between four adjacent corners $\underline{C}_{\{1gh\}}$, such as $\underline{C}_{(1gh)}$, $\underline{C}_{(1g-h)}$, $\underline{C}_{(g1h)}$, $\underline{C}_{(g1h)}$. Of the resulting four alternating edges two connect corners, such as $\underline{C}_{(1gh)}$ with $\underline{C}_{(1g-h)}$, at distances d_{h6} according to (124) while two connect corners, such as $\underline{C}_{(1gh)}$ with $\underline{C}_{(g1h)}$, at distances d_{h8} given by

$$d_{h8} = \sqrt{2} \left(2R_{100} - \sqrt{2} R_{110} \right). \quad (126)$$

The 8 $\{111\}$ facets are of the same hexagonal shape where each facet extends between six adjacent corners $\underline{C}_{\{1gh\}}$, such as $\underline{C}_{(1gh)}$, $\underline{C}_{(g1h)}$, $\underline{C}_{(h1g)}$, $\underline{C}_{(hg1)}$, $\underline{C}_{(gh1)}$, $\underline{C}_{(1hg)}$. Of the resulting six alternating edges three connect corners, such as $\underline{C}_{(1gh)}$ with $\underline{C}_{(g1h)}$, at distances d_{h8} according to (126) while three connect corners, such as $\underline{C}_{(1gh)}$ with $\underline{C}_{(1hg)}$, at distances d_{h7} according to (125).

Clearly, the largest distance from the polyhedral center to its surface along (a, b, c) directions, $s_{abc}(R_{100}, R_{110}, R_{111})$, equals the corresponding facet distance R_{abc} i.e.

$$s_{abc}(R_{100}, R_{110}, R_{111}) = R_{abc}. \quad (127)$$

Further, the area of each octagonal $\{100\}$ facet is given by F_0 where with (124) and (125)

$$F_0 = 4 \left(\sqrt{2} R_{110} - R_{100} \right)^2 - 2 \left(2\sqrt{2} R_{110} - R_{100} - \sqrt{3} R_{111} \right)^2 \quad (128)$$

and of each rectangular $\{110\}$ facet by F_1 where with (115) and (116)

$$F_1 = 2\sqrt{2} \left(\sqrt{3} R_{111} - \sqrt{2} R_{110} \right) \left(2R_{100} - \sqrt{2} R_{110} \right) \quad (129)$$

and of each hexagonal $\{111\}$ facet by F_2 where with (125) and (126)

$$F_2 = \sqrt{3} \left[\left(3R_{110} - \sqrt{6} R_{111} \right)^2 - (3/2) \left(2\sqrt{2} R_{110} - R_{100} - \sqrt{3} R_{111} \right)^2 \right]. \quad (130)$$

This yields the total facet surface, F_{surf} (sum over all facet areas) and the volume V_{tot} of the polyhedron according to

$$F_{\text{surf}} = 6F_0 + 12F_1 + 8F_2 \quad (131)$$

$$V_{\text{tot}} = (6F_0 R_{100} + 12F_1 R_{110} + 8F_2 R_{111}) / 3. \quad (132)$$

At the bottom of the inner region, i.e. for $R_{111} = R_{111}^b$ according to (102) the polyhedron $P(\underline{R}_{\{100\}}; \underline{R}_{\{110\}}; \underline{R}_{\{111\}})$ assumes a particular shape. The 12 $\{110\}$ facets of the polyhedron with R_{111} in the inner region are reduced to lines and there are only 6 $\{100\}$ and 8 $\{111\}$ facets as shown in figure 13. In fact, the polyhedron is described as cubo-octahedral $P(\underline{R}_{\{100\}}; \underline{R}_{\{111\}})$ of the truncated octahedral type ($R_{111}/R_{100} < 2/\sqrt{3}$) or of the cuboctahedral ($R_{111}/R_{100} = 2/\sqrt{3}$) type which has been discussed in detail in section 3.2.2.

There are two alternative intersection procedures to achieve a true non-generic polyhedron $P(\underline{R}_{\{100\}}; \underline{R}_{\{110\}}; \underline{R}_{\{111\}})$ which, however, lead to the same shapes and identical formulas for corner coordinates and all other structural parameters which have been discussed above. Therefore, they will be outlined only briefly in the following.

Intersecting cubo-octahedral $P(\underline{R}_{\{100\}}; \underline{R}_{\{111\}})$ with rhombohedral $P(\underline{R}_{\{110\}})$ polyhedra is achieved by fixing R_{100} and R_{111} with (99). Then the shape of $P(\underline{R}_{\{100\}}; \underline{R}_{\{110\}}; \underline{R}_{\{111\}})$ is fully determined by the size of its facet distance R_{110} . Here we distinguish between $P(\underline{R}_{\{100\}}; \underline{R}_{\{111\}})$ of the truncated octahedral and of the truncated cubic type according to (50a) and (50b). For truncated octahedral polyhedra, see

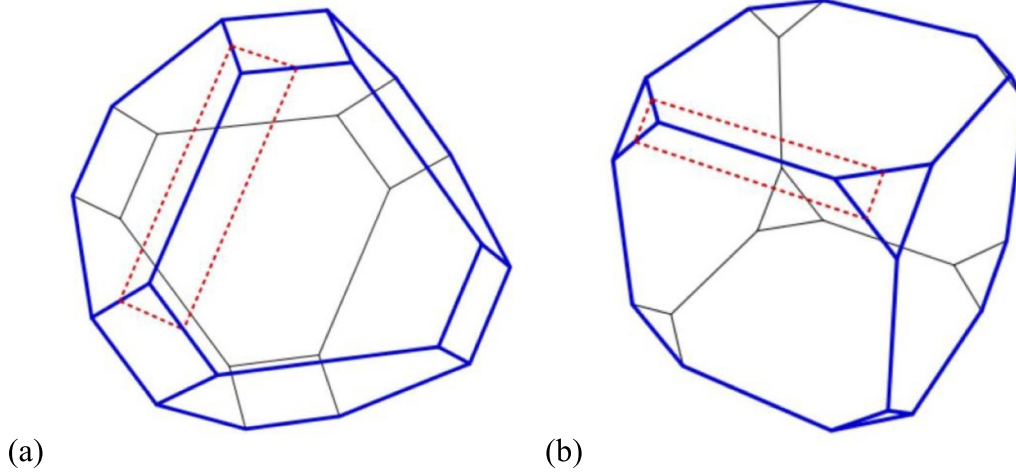


Figure 14. Sketch of cubo-octahedral polyhedra $P(\underline{R}_{\{100\}}; \underline{R}_{\{111\}})$, (a) truncated octahedral type, $R_{111}/R_{100} = 0.770$, $R_{110}/R_{100} = 0.943$, and (b) truncated cubic type, $R_{111}/R_{100} = 1.501$, $R_{110}/R_{100} = 1.414$, with front facets in blue and back facets in black. The dashed red rectangles show cuts along $\{110\}$ indicating the boundaries between outer and inner regions of the corresponding cubo-rhomb-octahedral polyhedra $P(\underline{R}_{\{100\}}; \underline{R}_{\{110\}}; \underline{R}_{\{111\}})$ for $R_{110} = R_{110}^s$ and (a) $R_{110}/R_{100} = 0.825$, (b) $R_{110}/R_{100} = 1.273$.

figure 14(a), and according to (97)–(99) R_{110} must always be within the range

$$\max(\sqrt{2/3} R_{111}, R_{100}/\sqrt{2}) \leq R_{110} \leq \sqrt{3/2} R_{111} \quad (133)$$

where there are two regions of different polyhedral shape,

$$\begin{aligned} \text{outer region : } R_{110}^s &\leq R_{110} \leq \sqrt{3/2} R_{111}, \\ R_{110}^s &= 1/\sqrt{8} (\sqrt{3} R_{111} + R_{100}) \end{aligned} \quad (134)$$

$$\begin{aligned} \text{inner region : } R_{110}^b &\leq R_{110} \leq R_{110}^s, \\ R_{110}^b &= \max(\sqrt{2/3} R_{111}, R_{100}/\sqrt{2}). \end{aligned} \quad (135)$$

For truncated cubic polyhedra, see figure 14(b), and according to (97)–(99) R_{110} must always be within the range

$$\max(\sqrt{2/3} R_{111}, R_{100}/\sqrt{2}) \leq R_{110} \leq \sqrt{2} R_{111} \quad (136)$$

where there are two regions of different polyhedral shape with (134) and (135),

$$\text{outer region : } R_{110}^s \leq R_{110} \leq R_{100}/\sqrt{2} \quad (137)$$

$$\text{inner region : } R_{110}^b \leq R_{110} \leq R_{110}^s. \quad (138)$$

As an illustration, figure 14 shows cubo-octahedral polyhedra $P(\underline{R}_{\{100\}}; \underline{R}_{\{111\}})$ of the truncated octahedral and truncated cubic type where the dashed red rectangles refer to cuts along $\{110\}$ indicating the boundaries between the outer and inner region of corresponding cubo-rhomb-octahedral polyhedra $P(\underline{R}_{\{100\}}; \underline{R}_{\{110\}}; \underline{R}_{\{111\}})$.

Intersecting rhombo-octahedral $P(\underline{R}_{\{110\}}; \underline{R}_{\{111\}})$ with cubic $P(\underline{R}_{\{100\}})$ polyhedra is achieved by fixing R_{110} and R_{111} with (98). Then the shape of $P(\underline{R}_{\{100\}}; \underline{R}_{\{110\}}; \underline{R}_{\{111\}})$ is fully

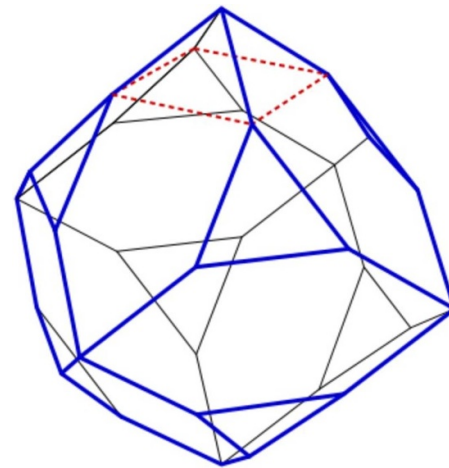


Figure 15. Sketch of rhombo-octahedral polyhedron $P(\underline{R}_{\{110\}}; \underline{R}_{\{111\}})$, $R_{110}/R_{111} = 0.942$, $R_{100}/R_{111} = 1.332$, with front facets in blue and back facets in black. The dashed red square shows a cut along $\{100\}$ indicating the boundary between the outer and inner region of corresponding cubo-rhomb-octahedral polyhedra $P(\underline{R}_{\{100\}}; \underline{R}_{\{110\}}; \underline{R}_{\{111\}})$ for $R_{100} = R_{100}^s$, $R_{100}/R_{111} = 0.933$, see text.

determined by the size of its facet distance R_{100} . According to (97)–(99) R_{100} must always be within the range

$$1/\sqrt{2} R_{110} \leq R_{100} \leq \sqrt{2} R_{110} \quad (139)$$

where there are two regions leading to different polyhedral shape,

$$\text{outer region : } R_{100}^s \leq R_{100} \leq \sqrt{2} R_{110}, \quad R_{100}^s = 2\sqrt{2} R_{110} - \sqrt{3} R_{111} \quad (140)$$

$$\text{inner region : } R_{100}^b \leq R_{100} \leq R_{100}^s, \quad R_{100}^b = 1/\sqrt{2} R_{110}. \quad (141)$$

As an illustration, figure 15 shows a rhombo-octahedral polyhedron $P(\underline{R}_{\{110\}}; \underline{R}_{\{111\}})$ where the dashed red square

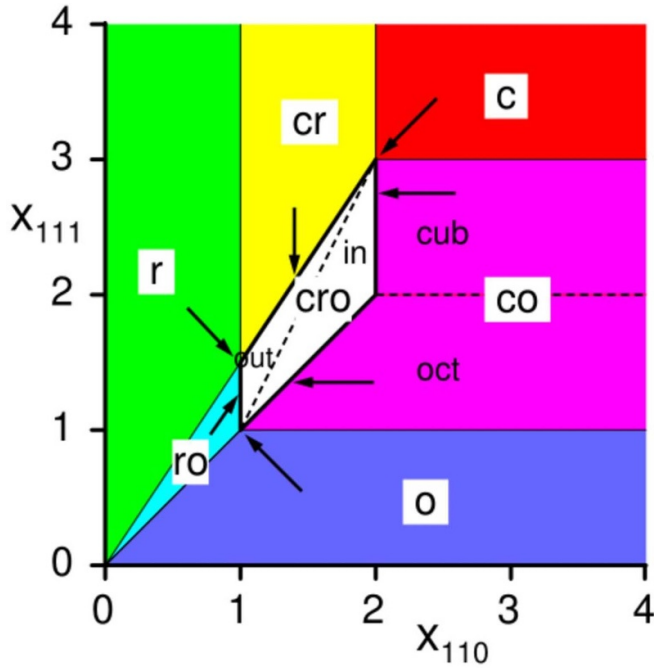


Figure 16. Phase diagram of all shapes of cubo-rhombic polyhedra $P(\underline{R}_{\{100\}}; \underline{R}_{\{110\}}; \underline{R}_{\{111\}})$ with x_{110} and x_{111} as order parameters. The different phases are shown by different colors and labeled accordingly. Arrows denote shift directions of shape identical polyhedra, see text.

shows a cut along $\{100\}$ indicating the boundary between the outer and inner region of corresponding cubo-rhombic polyhedra $P(\underline{R}_{\{100\}}; \underline{R}_{\{110\}}; \underline{R}_{\{111\}})$.

3.2.4.2. Classification of $P(\underline{R}_{\{100\}}; \underline{R}_{\{110\}}; \underline{R}_{\{111\}})$. The discussion in sections 3.2.1–3 and 3.2.4.1 allows a full classification of all shapes of polyhedra $P(\underline{R}_{\{100\}}; \underline{R}_{\{110\}}; \underline{R}_{\{111\}})$ with O_h symmetry according to the choice of the three facet distances $R_{100}, R_{110}, R_{111}$. First, we note that scaling $R_{100}, R_{110}, R_{111}$ by the same factor does not change the shape of a polyhedron. Thus, fixing R_{100} at any value allows to discriminate between all shapes by considering only two parameters derived from relative facet distances x_{110} and x_{111} where

$$x_{110} = \sqrt{2}R_{110}/R_{100}, \quad x_{111} = \sqrt{3}R_{111}/R_{100}. \quad (142)$$

This leads to a two-dimensional phase diagram with x_{110}, x_{111} as order parameters and shown in figure 16.

True cubo-rhombic polyhedra $P(\underline{R}_{\{100\}}; \underline{R}_{\{110\}}; \underline{R}_{\{111\}})$ are defined by (97)–(99) which converts to

$$1 < x_{110} < 2 \quad (143)$$

$$2/3x_{111} < x_{110} < x_{111} \quad (144)$$

$$1 < x_{111} < 3 \quad (145)$$

and corresponds to the central quadrangular area labeled ‘cro’ and confined by thick lines (cro phase) in figure 16. Here the

dashed line, defined according to (101) and converted to

$$x_{111} = 2x_{110} - 1 \quad (146)$$

separates polyhedra of the outer region (labeled ‘out’) from those of the inner region (labeled ‘in’).

True cubo-rhombic polyhedra $P(\underline{R}_{\{100\}}; \underline{R}_{\{110\}})$ are defined by (97) and (91) which converts to

$$1 < x_{110} < 2 \quad (147)$$

$$x_{111} \geq \min(3, 3/2x_{110}) = 3/2x_{110} \quad (148)$$

and corresponds to the infinite vertical strip labeled ‘cr’ (cr phase) in figure 16. Polyhedra of this phase along (vertical) lines of fixed x_{110} differ only by the size of the octahedral polyhedron $P(\underline{R}_{\{111\}})$ outside $P(\underline{R}_{\{100\}}; \underline{R}_{\{110\}})$. Therefore, they are identical with their counterparts at the cr/cro phase boundary obtained by vertical shifting according to

$$(x_{110}, x_{111}) \rightarrow (x_{110}, x_{111} = 3/2x_{110}) \quad (149)$$

in the phase diagram, see vertical arrow in figure 16.

True cubo-octahedral polyhedra $P(\underline{R}_{\{100\}}; \underline{R}_{\{111\}})$ are defined by (99) and (93) which converts to

$$1 < x_{111} < 3 \quad (150)$$

$$x_{110} \geq \min(2, x_{111}) \quad (151)$$

and corresponds to the infinite horizontal strip labeled ‘co’ (co phase) in figure 16. Here the dashed line, defined according to (50c) and converted to

$$x_{111} = 2 \quad (152)$$

separates polyhedra of the truncated octahedral type ($x_{111} \leq 2$, labeled ‘oct’) from those of the truncated cubic type ($x_{111} \geq 2$, labeled ‘cub’). Polyhedra of this phase along (horizontal) lines of fixed x_{111} differ only by the size of the rhombohedral polyhedron $P(\underline{R}_{\{110\}})$ outside $P(\underline{R}_{\{100\}}; \underline{R}_{\{111\}})$. Therefore, they are identical with their counterparts at the co/cro phase boundary obtained by horizontal shifting according to

$$(x_{110}, x_{111}) \rightarrow (x_{110} = x_{111}, x_{111}) \quad (\text{truncated octahedral}) \quad (153a)$$

$$(x_{110}, x_{111}) \rightarrow (x_{110} = 2, x_{111}) \quad (\text{truncated cubic}) \quad (153b)$$

in the phase diagram, see horizontal arrows in figure 16. In analogy, the dashed horizontal line inside the co phase refers to the same cubo-octahedral polyhedron for all x_{110} values which suggests a shift to the co/cro phase boundary according to

$$(x_{110}, x_{111} = 2) \rightarrow (x_{110} = 2, x_{111} = 2) \quad (\text{cuboctahedral}). \quad (153c)$$

True rhombo-octahedral polyhedra $P(\underline{R}_{\{110\}}; \underline{R}_{\{111\}})$ are defined by (78) and (95) which converts to

$$x_{110} < x_{111} < 3/2 x_{110} \quad (154)$$

$$\min(x_{110}, x_{111}) = x_{110} \leq 1 \quad (155)$$

and corresponds to the triangular area labeled ‘ro’ (ro phase) in figure 16. Polyhedra of this phase along (radial) lines of fixed x_{111}/x_{110} differ only by the size of the generic polyhedron $P(\underline{R}_{\{100\}})$ outside $P(\underline{R}_{\{110\}}; \underline{R}_{\{111\}})$. Therefore, they are identical with their counterparts at the ro/cro phase boundary obtained by radial shifting from the coordinate origin according to

$$(x_{110}, x_{111}) \rightarrow (x_{110} = 1, x_{111}/x_{110}) \quad (156)$$

in the phase diagram, see diagonal arrow in figure 16.

Generic cubic polyhedra $P(\underline{R}_{\{100\}})$ are defined by (31) and (45) which converts to

$$x_{110} \geq 2 \quad (157)$$

$$x_{111} \geq 3 \quad (158)$$

and corresponds to the infinite rectangular area labeled ‘c’ (c phase) in figure 16. Polyhedra of this phase are identical with their counterpart at the point

$$x_{110} = 2, x_{111} = 3 \quad (159)$$

(joining c, cr, cro, and co phases as indicated by an arrow in figure 16) since they differ only by the size of the generic rhombohedral and octahedral polyhedra outside $P(\underline{R}_{\{100\}})$.

Generic rhombohedral polyhedra $P(\underline{R}_{\{110\}})$ are defined by (32) and (75) which converts to

$$x_{100} \leq 1 \quad (160)$$

$$x_{111} \geq 3/2 x_{110} \quad (161)$$

and corresponds to the infinite vertical strip labeled ‘r’ (r phase) in figure 16. Polyhedra of this phase are identical with their counterpart at the point

$$x_{110} = 1, x_{111} = 3/2 \quad (162)$$

(joining r, ro, cro, and cr phases as indicated by an arrow in figure 16) since they differ only by the size of the generic cubic and octahedral polyhedra outside $P(\underline{R}_{\{110\}})$.

Generic octahedral polyhedra $P(\underline{R}_{\{111\}})$ are defined by (47) and (77) which converts to

$$x_{111} \leq 1 \quad (163)$$

$$x_{110} \geq x_{111} \quad (164)$$

and corresponds to the infinite horizontal strip labeled ‘o’ (o phase) in figure 16. Polyhedra of this phase are identical with their counterpart at the point

$$x_{110} = 1, x_{111} = 1 \quad (165)$$

(joining o, co, cro, and ro phases as indicated by an arrow in figure 16) since they differ only by the size of the generic cubic and rhombohedral polyhedra outside $P(\underline{R}_{\{111\}})$.

Altogether, the phase diagram shown in figure 16 covers all possible definitions of cubo-rhomb-octahedral polyhedra $P(\underline{R}_{\{100\}}; \underline{R}_{\{110\}}; \underline{R}_{\{111\}})$ where, however, polyhedra of truly different shape are already fully accounted for by x_{110}, x_{111} values inside the quadrangular area defined by (143)–(145) including its edges and corners which can be described as

$$1 \leq x_{110} \leq 2 \quad (166)$$

$$x_{110} \leq x_{111} \leq 3/2 x_{110}. \quad (167)$$

If the polyhedra are to limit NPs which represent sections with internal cubic bulk structure, as discussed previously [5], then facet distances R_{100}, R_{110} , and R_{111} assume discrete values due to the lattice periodicity. As a result, parameters x_{110} and x_{111} become fractional, forming a discrete periodic array of points inside the phase diagram where the periodicity cells are square for sc, rectangular 1×2 for fcc, and rectangular 2×1 for bcc lattices. Further, the cell size decreases with increasing NP size. This is illustrated in figure 17 showing the phase diagram of figure 16 with an added array of points, corresponding to an atom centered NP with internal fcc lattice. Here the facet distances are given by

$$\begin{aligned} R_{100} &= N a_o / 2, \quad R_{110} = M a_o a / (2\sqrt{2}), \\ R_{111} &= K a_o / \sqrt{3}, \quad N, M, K \text{ integer} \end{aligned} \quad (168)$$

with a_o denoting the lattice constant and hence according to (142)

$$x_{110} = M/N, \quad x_{111} = 2K/N \quad (169)$$

where in figure 17 the array refers to $R_{100} = 4a_o$, i.e. $N = 8$.

There are two alternative classification schemes of polyhedral shapes which are mentioned only briefly and discussed in detail in section S.2 of the supplement. First, fixing R_{110} at any value allows to discriminate between all shapes of polyhedra $P(\underline{R}_{\{100\}}; \underline{R}_{\{110\}}; \underline{R}_{\{111\}})$ by considering two parameters derived from relative facet distances y_{100} and y_{111} where

$$y_{100} = R_{100} / (\sqrt{2} R_{110}), \quad y_{111} = \sqrt{3} R_{111} / (\sqrt{2} R_{110}). \quad (170)$$

This leads to a two-dimensional phase diagram with y_{100}, y_{111} as order parameters and shown in figure 18(a). Second, fixing R_{111} at any value allows to discriminate between all shapes by considering two parameters derived from relative facet distances z_{100} and z_{110} where

$$z_{100} = R_{100} / (\sqrt{3} R_{111}), \quad z_{110} = \sqrt{2} R_{110} / (\sqrt{3} R_{111}) \quad (171)$$

This leads to a two-dimensional phase diagram with z_{100}, z_{110} as order parameters and shown in figure 18(b).

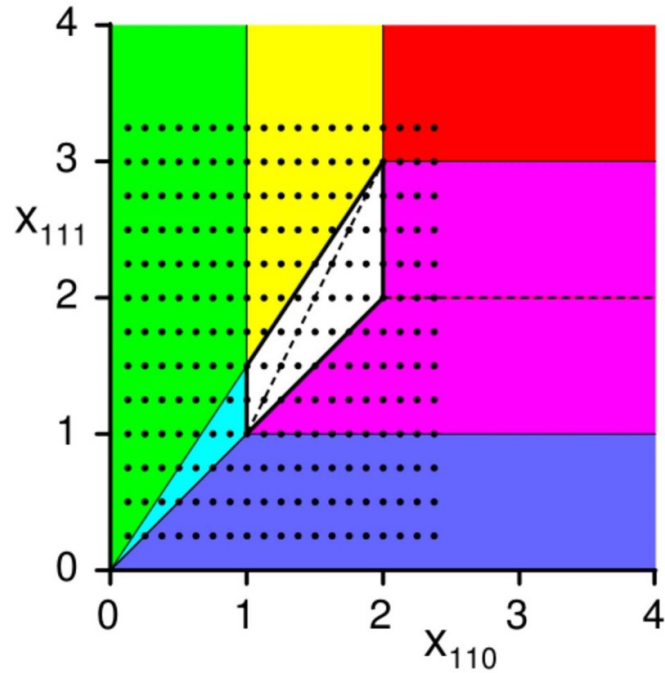


Figure 17. Phase diagram of all shapes of cubo-rhomb-octahedral polyhedra $P(\underline{R}_{\{100\}}; \underline{R}_{\{110\}}; \underline{R}_{\{111\}})$ with x_{110} and x_{111} as order parameters. The different phases are shown by colors identical with those of figure 16. The array of points illustrates possible values of x_{110} , x_{111} corresponding to a NP with internal fcc lattice and $R_{100} = 4a_0$, see text.

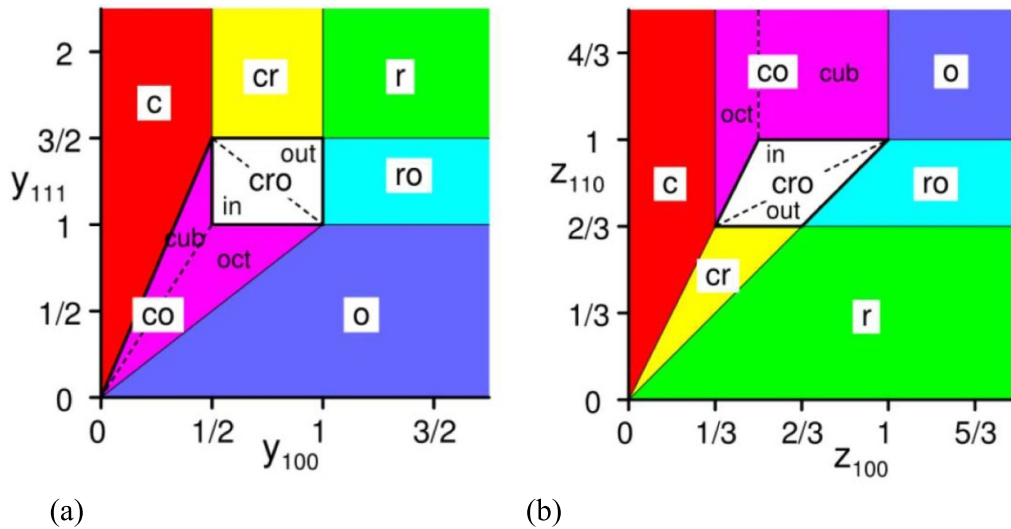


Figure 18. Phase diagram of all shapes of cubo-rhomb-octahedral polyhedra $P(\underline{R}_{\{100\}}; \underline{R}_{\{110\}}; \underline{R}_{\{111\}})$; (a) with y_{100} and y_{111} as order parameters, (b) with z_{100} and z_{110} as order parameters. The different phases are shown by different colors and labeled accordingly, see text.

4. Conclusions

The present theoretical analysis gives a full account of the shapes and structure of compact polyhedra with cubic O_h symmetry where all properties are discussed in analytical and numerical detail with visualization of characteristic examples. The polyhedral surfaces are described by facets representing planar sections with normal vectors along selected Cartesian directions (a, b, c) together with their O_h symmetry equivalents. Here we focus on facets reflecting normal directions of families $\{abc\} = \{100\}$, $\{110\}$, and $\{111\}$ which are

suggested for metal and oxide NPs with cubic lattices, representing sections of high-density monolayers of the cubic bulk. The structure evaluation identifies three types of generic polyhedra, cubic, rhombohedral, and octahedral (as special cases of hexoctahedral), which can serve for the description of non-generic polyhedra as intersections of corresponding generic species. Their structural properties are shown to be fully determined by only three structure parameters, facet distances R_{100} , R_{110} , and R_{111} of the three types of facets. In fact, all polyhedral shapes can already be characterized by only two relative facet distances, such as $x_{110} = \sqrt{2}R_{110}/R_{100}$

and $x_{111} = \sqrt{3}R_{111}/R_{100}$ which provides a novel phase diagram systematically classifying the polyhedra. If the polyhedra confine crystalline NPs forming sections with internal cubic bulk structure, then parameters x_{110} and x_{111} in the phase diagram become fractional to yield a discrete periodic array with square or rectangular periodicity cells where the cell size decreases with increasing NP size.

Further, structural properties of generic polyhedra of O_h symmetry, confined by facets with normal vectors of one general $\{abc\}$ family have been studied in analytical and numerical detail. These hexoctahedral polyhedra yield up to 48 facet directions and are shown to be fully characterized by only a facet distance R_{abc} and all facet indices, a , b , c , of the corresponding facet normal vector family $\{abc\}$.

Clearly, there is a multitude of other polyhedra of O_h symmetry with mixtures of facets that are described by different facet directions $\{abc\}$ not accounted for in this work and having to be dealt with separately in each case. Also, polyhedra of other symmetries, like hexagonal [21] or icosahedral [22, 23], need to be considered. However, the present results cover already the large set of polyhedra with cubic symmetry, which allows a unique systematic classification.

Altogether, the present analysis offers a sound basis to describe compact polyhedra of cubic symmetry which may be used as a repository available for NP simulations. Further, it can help the interpretation of structures of real compact NPs observed by experiment and can also stimulate further experimental research on nano- and mesoscopic particle structures, not identified so far.

Data availability statement

All data that support the findings of this study are included within the article (and any supplementary files).

ORCID iD

Klaus E Hermann  <https://orcid.org/0000-0002-3861-3916>

References

- [1] Cromwell P R 1999 *Polyhedra* (Cambridge University Press)
- [2] Träger F and Zu Putlitz G (eds) 1986 *Metal Clusters* (Springer)
- [3] Barhoum A and Makhlof A S H 2018 *Fundamentals of Nanoparticles: Classifications, Synthesis Methods, Properties and Characterization* (Elsevier)
- [4] Su D S, Zhang B and Schlögl R 2015 *Chem. Rev.* **115** 2818
- [5] Hermann K 2022 *Int. J. Nanosci.* **21** 2250010
- [6] Soloviev M 2012 *Nanoparticles in Biology and Medicine: Methods and Protocols* (Humana Press)
- [7] Silvestri N, Gavilán H, Guardia P, Brescia R, Fernandes S, Samia A C S, Teran F J and Pellegrino T 2021 *Nanoscale* **13** 13665–80
- [8] Egea-Benavente D, Diaz-Ufano C, Gallo-Cordova Á, Palomares F J, Lehman Cuya Huaman J, Barber D F, Del Puerto Morales M and Balachandran J 2023 *ACS Appl. Mater. Interfaces* **15** 32162–76
- [9] Gavilán H, Rizzo G M R, Silvestri N, Mai B T and Pellegrino T 2023 *Nat. Protocols* **18** 783–809
- [10] Olsson R T, Salazar-Alvarez G, Hedenqvist M S, Gedde U W, Lindberg F and Savage S J 2005 *Chem. Mater.* **17** 5109–18
- [11] Astruc D 2020 *Chem. Rev.* **120** 461–3
- [12] Liu L and Corma A 2018 *Chem. Rev.* **118** 4981–5079
- [13] Schwach P, Frandsen W, Willinger M-G, Schlögl R and Trunschke A 2015 *J. Catal.* **329** 560–73
- [14] Zalineeva A, Baranton S, Coutanceau C and Jerkiewicz G 2017 *Sci. Adv.* **3** e1600542
- [15] Cui C, Gan L, Li H-H, Yu S-H, Heggen M and Strasser P 2012 *Nano Lett.* **12** 5885–9
- [16] Rizo R and Roldan Cuenya B 2019 *ACS Energy Lett.* **4** 1484–95
- [17] Rizo R, Pérez-Rodríguez S and Garcia G 2019 *ChemElectroChem* **6** 4725–38
- [18] Zhou Z-Y, Tian N, Huang Z-Z, Chen D-J and Sun S-G 2008 *Faraday Discuss.* **140** 81–92
- [19] Altantzis T *et al* 2019 *Nano Lett.* **19** 477–81
- [20] Hermann K 2016 *Crystallography and Surface Structure, an Introduction for Surface Scientists and Nanoscientists* 2nd edn (Wiley)
- [21] Stoeva S I, Prasad B L V, Uma S, Stoimenov P K, Zaikovski V, Sorensen C M and Klabunde K J 2003 *J. Phys. Chem. B* **107** 7441–8
- [22] Zhang C, Zhang J, Han B, Zhao Y and Li W 2008 *Green Chem.* **10** 1094–8
- [23] Mayoral A, Barron H, Estrada-Salas R, Vazquez-Duran A and José-Yacamán M 2010 *Nanoscale* **2** 335–42
- [24] Lu Y, Zhang H, Wu F, Liu H and Fang J 2017 *RSC Adv.* **7** 18601–8
- [25] Eguchi M, Mitsui D, Wu H-L, Sato R and Teranishi T 2012 *Langmuir* **28** 9021–6
- [26] Krajczewski J, Kędziora M, Kołataj K and Kudelski A 2019 *RSC Adv.* **9** 18609–18
- [27] Broadhead E J, Monroe A and Moore Tibbetts K 2021 *Langmuir* **37** 3740–50
- [28] Radi A, Pradhan D, Sohn Y and Leung K T 2010 *ACS Nano* **4** 1553–60
- [29] Garnier E, Vidal-Iglesias F J, Feliu J M and Solla-Gullón J 2019 *Front. Chem.* **7** 527
- [30] Tian N, Zhou Z-Y, Sun S-G, Ding Y and Lin Wang Z 2007 *Science* **316** 732–5
- [31] Zhang F, Jin Q and Chan S-W 2004 *J. Appl. Phys.* **95** 4319–26
- [32] Bai Y, Yang T, Gu Q, Cheng G and Zheng R 2012 *Powder Technol.* **227** 35–42
- [33] Yang M, Zhub J-J and Li J-J 2004 *J. Cryst. Growth* **267** 283–7
- [34] Quan Z, Wang Y and Fang J 2013 *Acc. Chem. Res.* **46** 191–202
- [35] Hermann K 2022 Compact polyhedra of cubic symmetry: geometrical analysis and classification (arXiv:2209.08919) pp 1–43
- [36] Hermann K (C) 1991–2023 Balsac (build and analyze lattices, surfaces, and clusters), visualization and graphical analysis software (available at: www.fhi.mpg.de/th-department/software/klaushermann)
- [37] Ashcroft N W and Mermin N D 1976 *Solid State Physics* (Holt-Saunders International Editions)